

Title	細胞認識機能を有する神経細胞活動記録に向けた次世代微小電極技術の開発
Author(s)	羽賀, 渉
Citation	
Issue Date	2024-03
Type	Thesis or Dissertation
Text version	ETD
URL	<a href="http://hdl.handle.net/10119/19074">http://hdl.handle.net/10119/19074</a>
Rights	
Description	Supervisor: 筒井 秀和, 先端科学技術研究科, 博士

# Doctoral Dissertation

Development of next generation microelectrode  
technique toward neuronal activity recordings  
with cell recognition capability

WATARU HAGA

Supervisor: HIDEKAZU TSUTSUI

Graduate School of Advanced Science and Technology

Japan Advanced Institute of Science and Technology

Materials Science

2024 March

# Abstract

Molecules called synapse organizers are involved in the formation of synapses. Among them, clustering of neurexin-1 $\beta$  by interacting with neuroligin-1 is known to cause synaptogenesis. The ability of Neurexin-1 $\beta$  to induce synaptogenesis in synapse organizers has been studied from various viewpoints, and although the elucidation of this molecular function has been widely attempted, the use of this function as a molecular machine has not been quite common. In this study, I developed an engineered synapse organizer based on Neurexin-1 $\beta$  and established a method to fabricate a glass microelectrode in which the main body was insulated by glass and only the tip was metal (Gold). By combining these, I attempted to induce selective synaptogenesis in the glass microelectrode. The engineered synapse organizer we developed formed synapse-like structures on the surfaces of inorganic microbeads and glass microelectrodes by artificial binding, not intrinsic binding. The localization of synapsin, which acts as a synaptic marker molecule, and Rab3 in the introduced marker was consistent. The engineered synapse organizer we developed can be said to be capable of inducing synaptogenesis in the glass microelectrode. When the tips of microbeads and glass microelectrodes bearing Rab3 antibodies were contacted with neurons expressing Rab3, I confirmed the accumulation of Rab3 despite the binding by antibodies. The method for

fabricating the glass microelectrode was developed by preferentially selecting a tool that is universally used for the patch clamp method, which may be a compatible tool for fields that employ such electrophysiological measurement methods. I employed a focused ion beam (FIB) machine for the fabrication of the tip of the microelectrode, and I was able to perform highly reproducible fabrication. This allowed us to efficiently fabricate an electrode with an arbitrary tip shape using the FIB, if an electrode with gold conducting could be fabricated by a micropipette puller. Finally, in a proof-of-principle experiment using chick forebrain neurons, selective synaptogenesis was induced in the glass microelectrode in a non-CO<sub>2</sub>-dependent culture medium. Chick neurons are simple to culture, and unlike rats and other mammals, it is known that removing the forebrain neuron from an egg embryo is unlikely to cause biological problems.

Experiments showed that synaptogenesis by the engineered synapse organizer took at least 4 hours, but chick forebrain neurons transfected at room temperature and open air survived for at least 8 hours and formed synapses with antibody-modified microbeads and glass microelectrodes.

Keywords: Electrophysiology, Neuron, Synapse Organizer, Glass Microelectrode, Protein Adsorption

# Table of Contents

Abstract.....	0
Chapter 1 General Introduction.....	2
Chapter 2 Development of Engineered Synapse Organizer .....	21
Chapter 3 Development of Glass Microelectrodes with the Ability to Induce Synapse Formation .....	50
Chapter 4 Proof-of-Principle of Glass Microelectrodes with Selective Synaptic Induction Ability.....	90
General Discussion.....	110
Acknowledgements.....	117

# Chapter 1

## General Introduction

#### General purposes of this study

- Develop a synapse organizer-modified microelectrode to establish a microelectrode recording method with cell selectivity.

#### Previous study

- Measuring neuronal electrical activity using existing electrophysiological techniques (patch clamp and extracellular electrode methods). “NEHER, E., SAKMANN, B. (1976)”
- Synapse formation between an endogenous synaptic organizer (rat neuron) and a microelectrode arrays (MEA). “S. Kim et al. (2023)”
- Selective synaptogenic activity between modified microbeads by rat neuron (expressing engineered synapse organizers, NOT peptide-tag). “S.A. Hamid et al. (2023)”

Electrophysiology is a technique that can measure the electrical signals of neurons. By using this technique, we can understand how neurons and neurons transmit and process information, which can lead to the development of drugs that are useful in the treatment of neurological and psychiatric diseases. On the other hand, neurons are connected to each other by a structure called a synapse, and a signal is sent through the synapse. Each technique including the patch-clamp method, which is one of the electrophysiology techniques, can observe signals through synapses, but it is difficult to observe a specific synapse (it is possible to search for a "pair" by generating action potentials at the presynaptic region and searching for a synapse where the response can be seen, but it takes a huge amount of time). Therefore, we tried to demonstrate the principle of a new electrophysiology technique to connect an electrode and an arbitrary neuron by a synapse and directly observe signals from the synapse. The new electrophysiology technique proposed here uses a special molecule called a synaptic organizer that induces synaptic differentiation. It is known that this molecule causes synaptic differentiation when two pairs are connected to each other in the extracellular region, and recent research has discovered that it causes synapse formation even in inorganic materials other than neurons. It has also been found that even if the connecting part of the synaptic organizer (genetically modified Mouse NRXN-1 $\beta$  in previous research) is not



endogenous, as long as it is connected, synaptic differentiation starts from both ends. By combining these findings, we created a genetically modified synaptic organizer with a peptide tag in the extracellular region and tried to induce synapse formation on inorganic materials (microbeads and glass microelectrodes) modified with the ligand. The purpose of this study is to develop an engineered synaptic organizer-modified microelectrode and to conduct a proof-of-principle study to establish a microelectrode recording method with cell selectivity.

**The following is a description of the terms used in this paper, such as cell biology, electrophysiology, and molecular biology.**

## **1. Neurons**

In animals, including us humans, there are neurons that are responsible for information processing and transmission; neurons are electrically excitable and can generate action potentials that can be used as signals to transmit information to other neurons [1].

## **2. Axons and Dendrites**

Neurons consist of a cell body and two types of cytoplasmic processes that extend from

the cell body. One of these structures, the axon, transmits information to other neurons and muscles, while the other structure, the dendrite, receives information from other neurons. Although there is usually one axon per neuron, there are multiple dendrites [1, 2].

### **3. Neurons**

Neurons transmit electrical pulse signals on their axons that reach presynaptically to trigger the release of neurotransmitters that are received presynaptically to modulate the activity of ion channels. This neurotransmitter release is  $\text{Ca}^{2+}$ -dependent and is carried out by a molecular machinery centered on SNARE proteins (SNAREs are responsible for docking and fusion of synaptic vesicles to the active zone and the  $\text{Ca}^{2+}$ -triggering step itself in combination with the  $\text{Ca}^{2+}$  sensor synaptotagmin) [1]. The electrical signals received by the neurotransmitter are processed and become again electrical pulse signals, which are transmitted on other nerve cells [1, 3].

### **4. Synapses**

Charles S. Sherrington named the structures created at the junctions between neurons synapses. Synapses are the junctional structures where neurons communicate. Memory

and learning in the brain are expressed as changes in signal transmission through synapses (synaptic plasticity). There are about 1.000 billion neurons in the human brain, which are further connected to form a vast network [2]. Some synaptic transmissions involve the use of electricity and others involve the release of chemical substances; these are called electrical synapses and chemical synapses, respectively. A typical synaptic structure is shown below [4] (**fig. 1**)

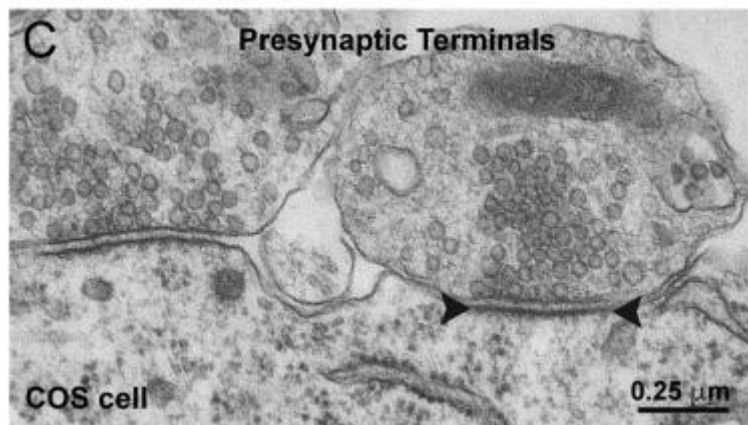


**Fig. 1.** A typical transmission electron micrograph of a synapse of a mouse neuron.

Structures such as postsynaptic density (PSD) and synaptic vesicles are visible.

## **5. Synapse Organizers**

Neurons are connected to other cells via synapses. The formation of synapses involves molecules called synapse organizers. Neuroligin, located in the postsynaptic membrane, was first described as a synapse organizer [2].

Synapse organizers are known to induce synaptic differentiation [5].

## **6. Variety of synapse organizers**

Synapse organizers are both pre - and postsynaptic and include Leukocyte common antigen-related receptor protein tyrosine phosphatases (LAR-RPTPs), LRRTMs, Cbln-GluR  $\delta$ , NGL-3, PTP  $\delta$ , Neurexin (NRXN), Neuroligin (NLGN), and PSD-95[6, 7, 8, 9,

10, 11, 12, 13].

## **7. Neurexin and Neuroligin**

Neurexins exist in the presynaptic neuronal membrane and are involved in the organization, and the maintenance of the synapses. The endogenous ligands for neurexins include neuroligins, which exist in the postsynaptic neuronal membrane.

These proteins are essential for synaptic transmission and play an important role in the organization of brain synapses. They act as cell adhesion molecules and are known to connect the pre-synapse and postsynapses [6, 7]. NRXN and NLGN couple through a trans-synaptic interaction in which the extracellular domain of NRXN on the presynaptic neuron binds to the extracellular domain of NLGN on the postsynaptic neuron, leading to the assembly of pre - and postsynaptic localized molecules such as synaptic vesicles and receptors required for synaptic function [14]. On the other hand, it has been suggested that NRXN and NLGN are important for synaptic function but are not required for synaptogenesis, and that the cytoplasmic tails of Neurexin are not required for synaptogenesis [6, 15].

## **8. Neurexin Family in Mammals**

Mammals have at least three neurexin genes, which are transcribed by two different promoters into longer  $\alpha$ -NRXN or shorter  $\beta$ -NRXN isoforms.

Furthermore,  $\alpha$ - and  $\beta$ -NRXN have five and two canonical alternative splice sites, respectively. These splice variants of NRXN can bind to NLGN but have selectivity NRXN-binding properties and regulate synaptogenesis in different ways. In addition,  $\alpha$ - and  $\beta$ -NRXN have five and two canonical alternative splice sites, respectively, and it is estimated that there are over 1000 variations of NRXN. Similarly, neuroligin is encoded by multiple genes and has alternative splice sites, resulting in diverse isoforms [14,16, 17, 18, 19, 20, 21, 22).

## **9. Coupling of NRXN and NLGN**

It has been shown that NRXN and NLGN signaling for pre-synaptic rigging occurs because dimerization of neuro-differentiating proteins located post-synaptically promotes clustering of NRXN located pre-synaptically [23, 24, 25, 26].

In addition, clustering of epitope-tagged NRXNs similarly triggers presynaptic differentiation, suggesting that clustering in some way is a prerequisite for presynaptic differentiation [24, 27].

## **10. Induction of Synaptogenesis in Non-biological Materials**

According to Yoshida et al., a synapse organizer (IL1RAPL1, PTP  $\delta$ ) can be used to form synaptic structures on magnetic microparticles (particle size ranging from 4.0 to 4.5  $\mu\text{l}$ ) [28] [. It has also been reported that NRXN  $\beta$  induces presynaptic differentiation in neurons derived from human induced pluripotent stem cells, and that NRXN  $\beta$  expressed in non-neuronal cells induces the accumulation of PSD-95, a postsynaptic marker molecule. Furthermore, when NLGN or LRRTM is expressed in non-neuronal cells, co-cultured neuronal cells form heterogeneous synapses with the cells [14, 15, 17, 29, 30, 31, 32]. Thus, induction of synaptogenesis by some synapse organizers has been found to be effective against non-neuronal cells expressing synapse organizers and non-biological materials [21, 22]. This suggests that synapse organizer molecules can be immobilized on the tip of the glass microelectrode prepared in this study (almost the same as the magnetic microparticle particle size used by Yoshida et al.), thereby sufficiently inducing synaptogenesis.

## **11. Patch Clamp Technique**

The patch-clamp technique is an electrophysiological recording method performed using glass electrodes. It is a powerful electrophysiological technique that can directly

measure membrane potential and the amount of current passing through the cell membrane, and is still a standard technique in electrophysiology and neuroscience [33].

The method was developed by Erwin Neher and Bert Sakmann, who won the Nobel Prize in Physiology or Medicine in 1991 for achieving precise recordings of the electrical current flowing through the cell membrane, which is associated with the opening and closing of a single ion channel [34].

## **12. Protein Adsorption**

Protein adsorption and immobilization on surfaces are influenced by several factors. These include the properties of the protein itself, the properties of the surface, and the environmental conditions in which the interaction occurs. Properties of the protein such as size, shape, charge, and hydrophobicity affect how the protein interacts with the surface. For example, a protein with a high surface charge is likely to adsorb to a surface with an opposite charge due to electrostatic attraction, and a protein with a hydrophobic region may preferentially adsorb to a hydrophobic surface [35, 36, 37].

It is also pointed out that the PI (Isoelectric Point) of the protein solution is one of the factors of adsorption, but it is not dominant, and the effect of water as a medium may be large [35, 38, 39].



### **13. Protein Adsorption on Metal Surfaces Under the Influence of Voltage/Electric Field**

It has been found that when a voltage is applied to electrodes in a protein solution, the protein is immobilized on its surface [35, 36, 37, 40, 41].

## References

- [1] 古市 貞一, 甘利 俊一. シリーズ脳科学 5—分子・細胞・シナプスから見る脳. 東京大学出版会, 2008.
- [2] 三品昌美, 分子脳科学 分子から脳機能と心に迫る. 化学同人, 2015.
- [3] 小澤 澗司, 福田 康一郎. 標準生理学 第8版. 医学書院, 2014.
- [4] T.C. Südhof, Towards an Understanding of Synapse Formation, *Neuron*. 100:276-293 (2018). <https://doi.org/10.1016/j.neuron.2018.09.040>.
- [5] K. Suzuki, J. Elegheert, I. Song, et al., A synthetic synapse organizer protein restores glutamatergic neuronal circuits, *Science* 369: eabb4853 (2020).  
<https://doi.org/10.1126/science.abb4853>.
- [6] T.C. Südhof, Neuroligins and neurexins link synaptic function to cognitive disease, *Nature*. 455 (2008) 903–911. <https://doi.org/10.1038/nature07456>.
- [7] A.M. Craig, Y. Kang, Neurexin-neuroligin signaling in synapse development, *Curr. Opin. Neurobiol.* 17 (2007) 43–52. <https://doi.org/10.1016/j.conb.2007.01.011>.
- [8] A.K. Lee, H. Khaled, N. Chofflet, et al., Synapse organizers in Alzheimer’s Disease: A Classification Based on Amyloid- $\beta$  Sensitivity, *Front. Cell. Neurosci.* 14 (2020) 1–16. <https://doi.org/10.3389/fncel.2020.00281>.
- [9] Y. Okuno, K. Sakoori, K. Matsuyama, et al., PTP $\delta$  is a presynapse organizer for the

formation and maintenance of climbing fiber to Purkinje cell synapses in the developing cerebellum, *Front. Mol. Neurosci.* 16: 1206245 (2023).

<https://doi.org/10.3389/fnmol.2023.1206245>.

[10] J.H. Trotter, C.Y. Wang, P. Zhou, et al., A combinatorial code of neurexin-3 alternative splicing controls inhibitory synapses via a trans-synaptic dystroglycan signaling loop, *Nat. Commun.* 14: 1771 (2023). <https://doi.org/10.1038/s41467-023-36872-8>.

[11] T.J. Siddiqui, A.M. Craig, Synaptic organizing complexes, *Curr. Opin. Neurobiol.* 21 (2011) 132–143. <https://doi.org/10.1016/j.conb.2010.08.016>.

[12] T. Zeppillo, H. Ali, S. Wenger, et al., Functional Neuroligin-2-MDGA1 interactions differentially regulate synaptic GABA A Rs and cytosolic gephyrin aggregation, *bioRxiv* (2022) doi:// 10.1101/2022.08.08.503083.

[13] S. Won, J.M. Levy, R.A. Nicoll, et al., MAGUKs: multifaceted synapse organizers, *Curr. Opin. Neurobiol.* 43 (2017) 94–101. <https://doi.org/10.1016/j.conb.2017.01.006>.

[14] C.I. Nam, L. Chen, Postsynaptic assembly induced by neurexin-neuroligin interaction and neurotransmitter, *PNAS* 102:6137-6142 (2005). [www.pnas.org/cgi/doi/10.1073/pnas.0502038102](http://www.pnas.org/cgi/doi/10.1073/pnas.0502038102).

- [15] O. Gokce, T.C. Südhof, Membrane-tethered monomeric neuexin LNS-domain triggers synapse formation, *J. Neurosci.* 33 (2013) 14617–14628.  
<https://doi.org/10.1523/JNEUROSCI.1232-13.2013>.
- [16] K. Tabuchi, T.C. Südhof, Structure and evolution of neuexin genes: Insight into the mechanism of alternative splicing, *Genomics.* 79 (2002) 849–859.  
<https://doi.org/10.1006/geno.2002.6780>.
- [17] A.A. Boucard, A.A. Chubykin, D. Comoletti, et al., A splice code for trans-synaptic cell adhesion mediated by binding of neuroligin 1 to  $\alpha$ - and  $\beta$ -neuexins, *Neuron.* 48 (2005) 229–236. <https://doi.org/10.1016/j.neuron.2005.08.026>.
- [18] F. Noborn, F.H. Sterky, Role of neuexin heparan sulfate in the molecular assembly of synapses – expanding the neuexin code?, *FEBS J.* 290 (2023) 252–265.  
<https://doi.org/10.1111/febs.16251>.
- [19] J. Dai, J. Aoto, T.C. Südhof, Alternative Splicing of Presynaptic Neuexins Differentially Controls Postsynaptic NMDA and AMPA Receptor Responses, *Neuron.* 102 (2019) 993-1008.e5. <https://doi.org/10.1016/j.neuron.2019.03.032>.
- [20] E.R. Graf, X. Zhang, S.X. Jin, et al., Neuexins induce differentiation of GABA and glutamate postsynaptic specializations via neuroligins, *Cell.* 119 (2004) 1013–1026.  
<https://doi.org/10.1016/j.cell.2004.11.035>.

- [21] M.F. Lisé, A. El-Husseini, The neuroligin and neurexin families: From structure to function at the synapse, *Cell. Mol. Life Sci.* 63 (2006) 1833–1849.  
<https://doi.org/10.1007/s00018-006-6061-3>.
- [22] S. Baudouin, P. Scheiffele, SnapShot: Neuroligin-neurexin complexes, *Cell*. 141: 908 (2010). <https://doi.org/10.1016/j.cell.2010.05.024>.
- [23] I.P. Fabrichny, P. Leone, G. Sulzenbacher, et al., Structural Analysis of the Synaptic Protein Neuroligin and Its  $\beta$ -Neurexin Complex: Determinants for Folding and Cell Adhesion, *Neuron*. 56 (2007) 979–991.  
<https://doi.org/10.1016/j.neuron.2007.11.013>.
- [24] S.L. Shipman, R.A. Nicoll, Dimerization of postsynaptic neuroligin drives synaptic assembly via transsynaptic clustering of neurexin, *Proc. Natl. Acad. Sci. U. S. A.* 109 (2012) 19432–19437. <https://doi.org/10.1073/pnas.1217633109>.
- [25] D. Araç, A.A. Boucard, E. Özkan, et al., Structures of Neuroligin-1 and the Neuroligin-1/Neurexin-1 $\beta$  Complex Reveal Specific Protein-Protein and Protein-Ca<sup>2+</sup> Interactions, *Neuron*. 56 (2007) 992–1003.  
<https://doi.org/10.1016/j.neuron.2007.12.002>.
- [26] Chen, X., Liu, H., Shim, A. et al. Structural basis for synaptic adhesion mediated by neuroligin-neurexin interactions. *Nat Struct Mol Biol* 15, 50–56 (2008).

<https://doi.org/10.1038/nsmb1350>

- [27] C. Dean, F.G. Scholl, J. Choih, et al., Neurexin mediates the assembly of presynaptic terminals, *Nature Neurosci.* 6: 708-716 (2003).  
<http://www.nature.com/natureneuroscience>.
- [28] T. Yoshida, M. Yasumura, T. Uemura, et al., IL-1 receptor accessory protein-like 1 associated with mental retardation and autism mediates synapse formation by trans-synaptic interaction with protein tyrosine phosphatase  $\delta$ , *J. Neurosci.* 31 (2011) 13485–13499. <https://doi.org/10.1523/JNEUROSCI.2136-11.2011>.
- [29] J.E. Kim, M.L. O’Sullivan, C.A. Sanchez, et al., Investigating synapse formation and function using human pluripotent stem cell-derived neurons, *Proc. Natl. Acad. Sci. U. S. A.* 108 (2011) 3005–3010. <https://doi.org/10.1073/pnas.1007753108>.
- [30] P. Scheiffele, J. Fan, J. Choih, et al., Neuroligin Expressed in Nonneuronal Cells Triggers Presynaptic Development in Contacting Axons, *Cell* 101: 657-669 (2000).
- [31] Z. Fu, P. Washbourne, P. Ortinski, et al., Functional Excitatory Synapses in HEK293 Cells Expressing Neuroligin and Glutamate Receptors, *J. Neurophysiol.* 90 (2003) 3950–3957. <https://doi.org/10.1152/jn.00647.2003>.
- [32] B. Chih, L. Gollan, P. Scheiffele., Alternative Splicing Controls Selective Trans-Synaptic Interactions of the Neuroligin-Neurexin Complex, *Neuron.* 51 (2006)

171–178. <https://doi.org/10.1016/j.neuron.2006.06.005>.

[33] 岡田 泰伸. 最新パッチクランプ実験技術法. 吉岡書店, 2011.

[34] NEHER, E., SAKMANN, B., Single-channel currents recorded from membrane of denervated frog muscle fibres. *Nature* 260, 799–802 (1976).

<https://doi.org/10.1038/260799a0>

[35] M. Rabe, D. Verdes, S. Seeger, Understanding protein adsorption phenomena at solid surfaces, *Adv. Colloid Interface Sci.* 162 (2011) 87–106.

<https://doi.org/10.1016/j.cis.2010.12.007>.

[36] B.H. Lapizco-Encinas, S. Ozuna-Chacón, M. Rito-Palomares, Protein manipulation with insulator-based dielectrophoresis and direct current electric fields, *J. Chromatogr. A.* 1206 (2008) 45–51. <https://doi.org/10.1016/j.chroma.2008.05.077>.

[37] M.A. Brusatori, Y. Tie, P.R. Van Tassel, Protein adsorption kinetics under an applied electric field: An optical waveguide lightmode spectroscopy study, *Langmuir.* 19 (2003) 5089–5097. <https://doi.org/10.1021/la0269558>.

[38] H. Noh, S. Yohe, E.A. Vogler, Volumetric Interpretation of Protein Adsorption: Ion-Exchange Adsorbent Capacity, Protein pI, and Interaction Energetics, *Biomaterials* 29: 2033-2048 (2008).

[39] P. Cha, A. Krishnan, V.F. Fiore, et al., Interfacial energetics of protein adsorption

from aqueous buffer to surfaces with varying hydrophilicity, *Langmuir*. 24 (2008)

2553–2563. <https://doi.org/10.1021/la703310k>.

[40] S. Takahashi, K. Kishi, R. Hiraga, et al., A new method for immobilization of his-

tagged proteins with the application of low-frequency AC electric field, *Sensors*

(Switzerland). 18: 784 (2018). <https://doi.org/10.3390/s18030784>.

[41] E.E. Htwe, Y. Nakama, Y. Yamamoto, et al., Adsorption characteristics of various

proteins on a metal surface in the presence of an external electric potential, *Colloids*

*Surfaces B Biointerfaces*. 166 (2018) 262–268.

<https://doi.org/10.1016/j.colsurfb.2018.03.035>.



## Chapter 2

# Development of Engineered Synapse Organizer

### Purpose of Chapter 2

- To develop small, engineered synapse organizers that do not cross-react with endogenous ligands.
- To establish an experimental culture system for proof of principle using microelectrodes.

### Achievement

- Using Neurexin-1 $\beta$ , synaptogenesis was confirmed by the binding of a small peptide tag between microbeads and chick or rat neurons.
- Synapse formation was confirmed for chick forebrain neurons within 4 hours at room temperature and in air.

### Remaining Challenges

- Search for the minimal functional unit for the active site of chick and mouse NRXN-1 $\beta$ .
- Confirmation of glutamine release at synapses formed by the developed engineered NRXN-1 $\beta$  to determine if they are functional synapses.

## Chapter 2 Key Points

- Neurexin-1 $\beta$  (b) without LNS (laminin, neurexin, sex hormone-binding globulin) domain exerts synaptogenesis via peptide-nanobody interactions
- The engineered synapse organizer functions in mammalian and chick forebrain neurons
- Chick neurons allow synaptogenesis in CO<sub>2</sub>-independent medium at room temperature
- Peptide-tag-based multiplexed organizers may be engineered with chick neurons

## **Introduction**

Membrane potential dynamics in neurons are thought to be fundamental to how neural circuits encode, process, and store information, though the details of these mechanisms remain one of the unsolved conundrums in science today. Technological development for detecting neuronal electrical activities in more detail is therefore essential. Despite recent advances in optical imaging approaches, the most stable readouts of electrical activity have been obtained with microelectrode techniques such as patch clamp, intracellular recording, and extracellular recording [1-3]. These techniques were originally suited for recording at a single or a few sites within a circuit, but recently developed flexible, arrayed electrodes are enabling large-scale parallel extracellular recording [4]. On the other hand, there are various technical limitations in the microelectrode-based activity recordings. One of the key limitations is that the recording target is, inherently, not specific to a cell type. The specificity is essential because neural circuits are composed of different cell types, each of which is believed to play a significant role in circuit function [5]. Researchers therefore need to identify the type of the cell under recording through various indirect means, such as visual identification of marker gene expression, dye injection followed by cell morphology inspection, waveform analysis, and so on. However, these identifications are not

compatible with large-scale parallel recordings.

We have been seeking to develop a neuron-microelectrode interface with inherent cell-type specificity by employing the molecular function of synapse organizers [6]. The synapse organizers are a series of membrane proteins that play a central role in the generation and maintenance of synapses, the junctions between neurons [7-9]. Specific sets of organizers in the axon and dendrite form complexes upon their contact, and trigger cellular signals to differentiate into pre- and post-synapses. Remarkably, such function of the synapse organizers is generally robust and is exerted even by contact with non-biological objects whose surfaces are modified with the organizers' receptor [10, 11]. Then, it is expected that a microelectrode functionalized with the receptor for synapse organizer is capable of exerting differentiation signals when in contact with a target neuron expressing that organizer and this leads to the formation of a synapse-like neuron-microelectrode junction but not with a non-target neuron, thereby establishing a cell type-specific interface (**Fig. 1**). We recently demonstrated that a gold microelectrode functionalized with Interleukin-1 receptor accessory protein-like 1 (IL1RAPL1) exerts such differentiation signals on the cortical neurons contacted [6]. There, IL1RAPL1 is a natural synapse organizer in the postsynaptic membrane and interacts with PTP $\delta$ , a synapse organizer in the presynaptic membrane [12, 13]. Since

these natural synapse organizers are pre-existing in neurons, it is necessary to develop engineered organizers that do not interact with the natural organizers to avoid interference and achieve a cell-type-specific neuron-microelectrode junction (**Fig. 1**). Neurexin-1 $\beta$  (NRXN-1 $\beta$ ), another natural synapse organizer in the presynaptic membrane, could serve as a molecular platform for this purpose [14]. The endogenous receptors for NRXN-1 $\beta$  include neuroligin-1 (Nlgn1) in the postsynaptic membrane. When NRXN-1 $\beta$  and Nlgn1 come into contact and form a trans-cellular complex, as Nlgn1 is a dimer-forming protein, clustering of Nrnx1 is promoted and this clustering then triggers a cellular signal for presynaptic differentiation [10, 15]. Importantly, the sub-region of NRXN-1 $\beta$  recognized by the receptor and that for triggering differentiation signal is structurally independent [14]. Therefore, a modified NRXN-1 $\beta$ , in which the recognition region is replaced by an artificial ligand, is expected to exert synaptogenic activity following its clustering driven by specific ligand-receptor interactions. The previous work showed that a variant of green fluorescence protein functions as such an artificial ligand [14]. But the ~27 kD fluorescent protein is relatively a large ligand. In general, small molecular tools are advantageous from the viewpoint of gene delivery and expression. Also, conditions required for synaptogenic activities, which provide important information for future prototyping of the synapse

organizer-based microelectrode technology, have yet to be fully addressed. We, therefore, set the purposes of this study as the generation and characterization of compact engineered synapse organizers.

## **Material and Methods**

### *Molecular biology*

DNA constructions were performed with the standard PCR-based cloning techniques.

For PCR, ligation, and plasmid purification, we used PrimeSTAR Max DNA polymerase, DNA Ligation Kit Ver.1, and NucleoBond Xtra Midi Kit, respectively. All these products are from Takara Bio (Shiga, Japan).

### *Cell culture*

HEK293T cells were cultured in Dulbecco's Modified Eagle Medium (Fujifilm, Tokyo, Japan) supplemented with 10% fetal bovine serum (FBS) (Thermo Fisher Scientific, MA, USA). Primary cortical neurons were prepared from Wister rat embryos on embryonic day 18 as described elsewhere [16, 17], and were cultured in minimum essential medium (MEM) (Sigma M4655, MO, USA) supplemented with 2% FBS and 1% B27 (Thermo Fisher Scientific, MA, USA). For the preparation of chick forebrain

neurons, we established the following procedure which is modified from the previous reports [18, 19]. Briefly, fertilized chicken eggs purchased from a local distributor were incubated for 8~9 days at 38 °C. The forebrains were collected in 2 ml ice-cold PBS without divalent cations. After careful removal of the meninges under a dissecting microscope, the brain tissue was mechanically chopped with a surgical blade into small pieces less than 0.5 mm, treated with 0.05% trypsin (Nacalai Tesque, Kyoto, Japan) in PBS(-) containing 10 unit of DNAaseI (Takara Bio, Shiga, Japan) for 7 minutes, triturated with a pipette, and filtered through a 100 µm mesh cell strainer. Dissociated neurons were centrifuged at 1000 rpm for 10 minutes, re-suspended with minimum essential medium (MEM) (Sigma M4655, MO, USA) supplemented with 2 % FBS and 1 % B27 (Thermo Fisher Scientific, MA, USA), and plated onto φ 12 mm coverslips coated with a mixture of equal volumes of poly-L-lysine (1.0 mg/ml) and poly-D-lysine (0.1 mg/ml). On the next day, the culture medium was replaced with minimum essential medium supplemented with 2 % horse serum and 1 % B27. Plasmid transfection to the rat hippocampal and chick forebrain neurons was performed at DIV (days in-vitro) 6 and 4, respectively, using Lipofectamine 3000 reagent (Thermo Fisher Scientific, MA, USA) according to the manufacturer's protocol. All animal experiments followed ARRIVE guidelines. Thirty-two rat embryos



from three pregnant rats and 25 chicken embryos from the fertilized eggs were used for experiments relevant to this study, including various tests. The sex of embryos was not distinguished. Experimental animals were used along the institutional guidelines for the care of animals provided by Japan Advanced Institute of Science and Technology as well as the National Institutes of Health guide for the care and use of Laboratory animals.

#### *Evaluation of the synaptogenic activities*

The synaptogenic activities of the engineered synapse organizers were evaluated by the microbeads assay. Synthetic cDNA encoding anti-BC2 nanobody (anti-SpotNb) was designed (Integrated DNA Technologies, IA, USA), sub-cloned into an Fc fusion protein expression vector, and transfected into HEK293T cells. The FBS concentration in the culture medium of HEK cells was reduced to 2%, into which the anti-SpotNb-Fc fusion protein was secreted. The medium was harvested, passed through a 0.22  $\mu\text{m}$  pore syringe filter (Advantech, Tokyo, Japan), and incubated with protein-A magnetic microbeads ( $\phi \sim 4.7 \mu\text{m}$ , PAMS-40-S, Spherotech, IL, USA) in a low protein binding micro-centrifuge tubes at 4 °C for overnight. Typically, 15  $\mu\text{l}$  beads solution was incubated with  $\sim 10 \mu\text{g}$  anti-SpotNb-Fc fusion protein. The protein-conjugated

microbeads were deeply washed with neuron culture medium and transferred onto the neuron culture, typically at the density of  $10^5$  beads per a  $\phi$  12 mm coverslip of neuron culture. Leiboviz L15 based medium was used for the experiments to investigate the time and CO<sub>2</sub> dependence of chick forebrain neurons as described below. After a defined co-culture time (1~20 hours), neurons were fixed and subjected to confocal microscopy imaging (FV1000D, Olympus, Tokyo, Japan).

## Results

The primary structure of NRXN-1 $\beta$  consists of an N-terminal signal peptide (SP), an LNS (i.e., laminin, neurexin, sex hormone-binding globulin) domain, a transmembrane domain (TM), and a PDZ domain binding motif at the C-terminal cytoplasmic end (**Fig. 2a**). The LNS domain is known to constitute the binding interface with Nlgn1 [10]. To design a compact engineered organizer, I tested whether Spot-tag could act as a ligand to promote clustering. Spot-tag is a 1.4 kD peptide, PDRVRAVSHWSS in the single-letter code, and is an improved ligand for the anti-BC2 nanobody [20, 21]. To avoid confusion due to its name, here I refer to anti-BC2 nanobody as anti-SpotNb. We modified mouse NRXN-1 $\beta$  (Sequence ID: NP\_001333889.1) to lack the LNS domain, have a Spot-tag downstream of the signal peptide and Flag-tag, and also a presynaptic

marker, EGFP-Rab3, via a self-cleaving P2A peptide, and named Spot-mNRXN-1 $\beta$  $\Delta$ ECD::P2A-EGFP-Rab3 (**Fig. 2a**). Flag-tag was not used in the present study. Gene transfer efficiency in primary cultured neurons is generally limited by standard lipofection methods. Therefore, to observe a sufficient number of contacts between the objects and the transfected neurons, magnetic microbeads conjugated with protein A (PAMS-40-S, Spherotech, Illinois, USA) were used to emulate microelectrodes (**Fig. 2b**). Rat cortical neurons were plated onto  $\phi$  12 mm coverslips, transfected with Spot-mNRXN-1 $\beta$  $\Delta$ ECD::P2A-EGFP-Rab at 6 days *in vitro* culture, and the next day, anti-SpotNb decorated microbeads were added and co-cultured overnight. Neurons expressing this construct were easily identified by fluorescence derived from EGFP-Rab3. Accumulations of EGFP-Rab3 signals were often observed at the sites of contact between the axon and the microbead, which showed synaptogenic activities mediated through the peptide-nanobody interaction (**Fig. 2c**). In the control experiments in which the rat cortical neurons were co-cultured with the undecorated microbeads, no such accumulations of EGFP-Rab3 were found at the sites of contact (**Fig. 2d**). Then, I examined whether Spot-mNRXN-1 $\beta$  $\Delta$ ECD::P2A-EGFP-Rab3 could exhibit synaptogenic activity in the chick forebrain neuron culture. This is because primary cultures of chick forebrain neurons growing into typical pyramidal shapes can be

prepared in a rapid procedure and maintained in a CO<sub>2</sub>-independent culture medium [18, 19], which should be useful for the future development of the synapse-organizer-based bioelectronic interface. Following co-culture of chick forebrain neurons expressing Spot-mNRXN-1βΔECD::P2A-EGFP-Rab3 and the microbeads decorated with anti-SpotNb, I did observe accumulation of EGFP-Rab3 signals were found at the sites of contact (**Fig. 2e**). Then, again as a negative control, the cortical neurons expressing a construct in which Spot-tag has been substituted with a chromophore deficient variant of fluorescence protein (Venus\_Y66G, or YFP<sub>null</sub>; [22]) were co-cultured with the microbeads. Rab3 signals were not observed (**Fig. 2f**), which ensured that the Rab3 signals are not directly caused by the anti-SpotNb decorated microbeads but reflect the association between the ligand (i.e. Spot-tag) and the receptor (i.e. anti-SpotNb). To statistically confirm these trends, I defined an index of Rab3 accumulation as  $I_{\text{bead}}/I_{\text{axon}}-1$ , where  $I_{\text{bead}}$  and  $I_{\text{axon}}$  are the integrals of the EGFP signal in a 50 μm<sup>2</sup> circular region around the beads and that around the representative axons not in contact with the beads, respectively, and named as the Rab3 index. The Rab3 index was analyzed for the laser scanning microscopy images taken under identical imaging conditions. It was confirmed that the accumulations of Rab3 were statistically significant both to the two negative controls (**Fig. 2g**).

Next, I sought to examine whether the use of NRXN-1 $\beta$  derived from the chick protein database could result in similar or any further enhancement in the synapse-inducing activity. After searching the National Center for Biotechnology Information database, we focused on *Gallus gallus* NRXN-1 $\beta$  (Sequence ID: NP\_001185905.1) and generated a construct named Spot-cNRXN-1 $\beta$  $\Delta$ ECD::P2A-EGFP-Rab3 which again lacks the extracellular LNS domain to prevent interaction with the natural ligands (**Fig. 3a**). The resulting construct contained 7 amino acid mismatches compared to the mouse NRXN-1 $\beta$ -based construct (**Fig. S1**). Synaptogenic activities were evaluated with microbead assays in rat cortical and chick forebrain neurons. In both types of neurons when contacted with microbeads decorated with anti-SpotNb, synaptogenic activity similar to that observed with mouse neurexin-derived sequences was observed (**Fig. 3b, c**), but not with the control bare microbeads (**Fig. 3d**). The trend was also confirmed through the image analysis (**Fig. 3e**). Thus, it was found that the mouse and chick Nrnx1-derived engineered synapse organizers are compatible in their synaptogenic activity in rat cortical and chick forebrain neurons. In both cortical neurons and chick forebrain neurons, there was no significant difference in the strength of synaptic induction between Spot-mNRXN-1 $\beta$  $\Delta$ ECD::P2A-EGFP-Rab3 and Spot-cNRXN-1 $\beta$  $\Delta$ ECD::P2A-EGFP-Rab3.

Our particular future direction is to exploit the neuron-microelectrode junction formed with the engineered synapse organizer as a bioelectronic interface. Knowledge of the time, temperature, and atmospheric conditions required for synapse induction against the objects will be essential for future research and development. I addressed these issues using chick forebrain neurons because of the advantages mentioned above. The time required for induction was investigated by fixing the chick forebrain neurons transfected with Spot-cNRXN-1 $\beta$  $\Delta$ ECD::P2A-EGFP-Rab3 after different times of co-culture with the microbeads decorated with anti-SpotNb. The effects of atmosphere and temperature were investigated by performing the co-culture in the medium based on minimum essential medium (MEM) at 37 °C, Leibovitz's L15 medium at 37 °C, and L15 medium at room temperature (25 °C). Here, MEM is a CO<sub>2</sub>-dependent culture medium, used in the presence of 5% CO<sub>2</sub>, and L15 is a CO<sub>2</sub>-independent medium, used under the normal atmospheric condition. All the culture medium was supplemented with 2% horse serum. After 2 hours, Rab3 accumulations were not typically observed, although were seen infrequently. (Fig. 4a, Fig. S2). After 4, 8, and 12 hours of the co-culture, Rab3 accumulations were more common at the sites of contact between axon and microbeads in all of these conditions (**Fig. 4a**). As confirmed by the analysis of the Rab3 index (**Fig. 4b**), the induction efficacy tended to increase with time gradually, but

there were no significant differences in the Rab3 index between MEM and L15 media and between 37°C and 25°C.

## **Discussion**

In this study, we developed Spot-tag-based compact engineered synapse organizers using NRXN-1 $\beta$  sequences derived from mouse or chick genes. Both of these organizers showed synaptogenesis in rat cortical neurons and chick forebrain neurons upon contact with objects decorated with anti-SpotNb. The results suggested three major implications.

The first is on the utility of using a peptide tag. Since several different combinations of short peptide tags and their specific nanobodies have been developed [23, 24], the successful induction of the presynaptic structure through the interaction of Spot-tag with its nanobody opens the possibility of further developing multiple engineered synapse organizers and their specific activators. Such a set of orthogonal molecular tools is expected to realize a multiplexed molecularly induced bioelectronics interface, as well as modification of neural circuits at unprecedented levels of detail. Furthermore, owing to the small ligand size, the total cDNA sequences for the engineered organizer and the downstream presynapse marker (i.e. EGFP-Rab3) do not exceed 2k base pairs, the

practical limit of cDNA size for packaging into adeno-associated virus (AAV) vectors. It is expected that the gene transfer efficiency will be improved with the use of AAV vectors, which is of practical importance in increasing lab work efficiency.

The second is on NRXN-1 $\beta$  itself. There were seven mismatches between the sequences comprising the transmembrane and cytoplasmic regions of mouse and chick NRXN-1 $\beta$  used in this study (**Fig. S1**), but no clear differences in the synaptogenic activity of these proteins were found in rat cortical and chick forebrain neurons, at least by the evaluations with EGFP-Rab3. Thus, the region of NRXN-1 $\beta$  responsible for the induction signaling of synaptogenesis is conserved and appears to function universally and even across species. This trend is in sharp contrast to the high specificity with which NRXN-1 $\beta$  forms transcellular heterophilic complexes with its ligand in the extracellular space. The observed universality may be explained by the relatively conserved amino acid sequence of the cytoplasmic region of mouse and chick NRXN-1 $\beta$  with the PDZ domain binding motif at its end, but, on the other hand, the previous study has shown that the cytoplasmic region of NRXN-1 $\beta$  is not necessarily required for exerting the induction signal [25]. Understanding the core region responsible for the induction as well as the downstream molecular mechanism would be one of the important future directions.



The third is on the practical advantages of chick forebrain neurons. The results indicated that there is a high degree of compatibility between rat cortical neurons and chick forebrain neurons concerning synaptogenic activities by the NRXN-1 $\beta$ -based engineered synapse organizers. This is not simply explained only by the structural similarity of NRXN-1 $\beta$  but suggests the conserved molecular mechanisms that detect its clustering and activate the downstream signal cascade for differentiation. In addition to the benefits that the experiments of forming neuron-object junctions can be conducted under air atmosphere typically in  $\sim$ 4 hours, the culture of chick forebrain neurons has several practical advantages over mammalian neurons, including a rapid and inexpensive procedure and fewer concerns regarding the use of laboratory animals. Thus, the chick forebrain neurons expressing the engineered synapse organizers developed in the present work would serve as a useful cellular model for establishing the molecularly-inducible neuron-microelectrode interface and also for developing molecular tools for neural circuit editing.

## References

- [1] Malmivuo, Jaakko, and Robert Plonsey, *Bioelectromagnetism: Principles and Applications of Bioelectric and Biomagnetic Fields* (New York, 1995; online edn, Oxford Academic, 22 Mar. 2012), <https://doi.org/10.1093/acprof:oso/9780195058239.001.0001>.
- [2] Nicholls, J. G., Martin, A. R., Fuchs, P. A., Brown, D. A., Diamond, M. E., & Weisblat, D. A. (2012). *From neuron to brain* (5th ed.). Sinauer Associates.
- [3] Colin Leech; *Microelectrode Techniques: The Plymouth Workshop Handbook*. *J Cell Sci* 1 June 1988; 90 (2): 192. doi: <https://doi.org/10.1242/jcs.90.2.192>
- [4] J.J. Jun, N.A. Steinmetz, J.H. Siegle, D.J. Denman, M. Bauza, B. Barbarits, A.K. Lee, C.A. Anastassiou, A. Andrei, Ç. Aydin, M. Barbic, T.J. Blanche, V. Bonin, J. Couto, B. Dutta, S.L. Gratiy, D.A. Gutnisky, M. Häusser, B. Karsh, P. Ledochowitsch, C.M. Lopez, C. Mittelut, S. Musa, M. Okun, M. Pachitariu, J. Putzeys, P.D. Rich, C. Rossant, W.L. Sun, K. Svoboda, M. Carandini, K.D. Harris, C. Koch, J. O’Keefe, T.D. Harris, Fully integrated silicon probes for high-density recording of neural activity, *Nature*. 551 (2017) 232–236. <https://doi.org/10.1038/nature24636>.
- [5] R. Yuste, M. Hawrylycz, N. Aalling, A. Aguilar-Valles, D. Arendt, R.A. Arnedillo, G.A. Ascoli, C. Bielza, V. Bokharaie, T.B. Bergmann, I. Bystron, M.

Capogna, Y. Chang, A. Clemens, C.P.J. de Kock, J. DeFelipe, S.E. Dos Santos, K. Dunville, D. Feldmeyer, R. Fiáth, G.J. Fishell, A. Foggetti, X. Gao, P. Ghaderi, N.A. Goriounova, O. Güntürkün, K. Hagihara, V.J. Hall, M. Helmstaedter, S. Herculano, M.M. Hilscher, H. Hirase, J. Hjerling-Leffler, R. Hodge, J. Huang, R. Huda, K. Khodosevich, O. Kiehn, H. Koch, E.S. Kuebler, M. Kühnemund, P. Larrañaga, B. Lelieveldt, E.L. Louth, J.H. Lui, H.D. Mansvelder, O. Marin, J. Martinez-Trujillo, H. Moradi Chameh, A. Nath, M. Nedergaard, P. Němec, N. Ofer, U.G. Pfisterer, S. Pontes, W. Redmond, J. Rossier, J.R. Sanes, R. Scheuermann, E. Serrano-Saiz, J.F. Steiger, P. Somogyi, G. Tamás, A.S. Tolia, M.A. Tosches, M.T. García, H.M. Vieira, C. Wozny, T. V. Wuttke, L. Yong, J. Yuan, H. Zeng, E. Lein, A community-based transcriptomics classification and nomenclature of neocortical cell types, *Nat. Neurosci.* 23 (2020) 1456–1468. <https://doi.org/10.1038/s41593-020-0685-8>.

[6] S. Kim, M. Imayasu, T. Yoshida, H. Tsutsui, Formation of neuron-microelectrode junction mediated by a synapse organizer, *Appl. Phys. Express.* 16 (2023). <https://doi.org/10.35848/1882-0786/acd166>.

[7] T.J. Siddiqui, A.M. Craig, Synaptic organizing complexes, *Curr. Opin. Neurobiol.* 21 (2011) 132–143. <https://doi.org/10.1016/j.conb.2010.08.016>.

[8] H. Takahashi, A.M. Craig, Protein tyrosine phosphatases PTP $\delta$ , PTP $\zeta$ , and

LAR: Presynaptic hubs for synapse organization, *Trends Neurosci.* 36 (2013) 522–534. <https://doi.org/10.1016/j.tins.2013.06.002>.

[9] T.J. Siddiqui, R. Pancaroglu, Y. Kang, A. Rooyakkers, A.M. Craig, LRRTMs and neuroligins bind neurexins with a differential code to cooperate in glutamate synapse development, *J. Neurosci.* 30 (2010) 7495–7506. <https://doi.org/10.1523/JNEUROSCI.0470-10.2010>.

[10] C. Dean, F.G. Scholl, J. Choih, S. DeMaria, J. Berger, E. Isacoff, P. Scheiffele, Neurexin mediates the assembly of presynaptic terminals, *Nat. Neurosci.* 6 (2003) 708–716. <https://doi.org/10.1038/nn1074>.

[11] T. Yoshida, M. Yasumura, T. Uemura, S.J. Lee, M. Ra, R. Taguchi, Y. Iwakura, M. Mishina, IL-1 receptor accessory protein-like 1 associated with mental retardation and autism mediates synapse formation by trans-synaptic interaction with protein tyrosine phosphatase  $\delta$ , *J. Neurosci.* 31 (2011) 13485–13499. <https://doi.org/10.1523/JNEUROSCI.2136-11.2011>.

[12] T. Yoshida, T. Shiroshima, S.J. Lee, M. Yasumura, T. Uemura, X. Chen, Y. Iwakura, M. Mishina, Interleukin-1 receptor accessory protein organizes neuronal synaptogenesis as a cell adhesion molecule, *J. Neurosci.* 32 (2012) 2588–2600. <https://doi.org/10.1523/JNEUROSCI.4637-11.2012>.

- [13] T. Yoshida, A. Yamagata, A. Imai, J. Kim, H. Izumi, S. Nakashima, T. Shiroshima, A. Maeda, S. Iwasawa-Okamoto, K. Azechi, F. Osaka, T. Saitoh, K. Maenaka, T. Shimada, Y. Fukata, M. Fukata, J. Matsumoto, H. Nishijo, K. Takao, S. Tanaka, S. Okabe, K. Tabuchi, T. Uemura, M. Mishina, H. Mori, S. Fukai, Canonical versus non-canonical transsynaptic signaling of neuroligin 3 tunes development of sociality in mice, *Nat. Commun.* 12 (2021) 1–15. <https://doi.org/10.1038/s41467-021-22059-6>.
- [14] S.A. Hamid, M. Imayasu, T. Yoshida, H. Tsutsui, Epitope-tag-mediated synptogenic activity in an engineered neurexin-1 $\beta$  lacking the binding interface with neuroligin-1, *Biochem. Biophys. Res. Commun.* 658 (2023) 141–147. <https://doi.org/10.1016/j.bbrc.2023.03.063>.
- [15] S.L. Shipman, R.A. Nicoll, Dimerization of postsynaptic neuroligin drives synaptic assembly via transsynaptic clustering of neurexin, *Proc. Natl. Acad. Sci. U. S. A.* 109 (2012) 19432–19437. <https://doi.org/10.1073/pnas.1217633109>.
- [16] A.H. Kossel, C. V. Williams, M. Schweizer, S.B. Kater, Afferent innervation influences the development of dendritic branches and spines via both activity-dependent and non-activity-dependent mechanisms, *J. Neurosci.* 17 (1997) 6314–6324. <https://doi.org/10.1523/jneurosci.17-16-06314.1997>.

- [17] Y. Kakinuma, H. Hama, F. Sugiyama, K. Goto, K. Murakami, A. Fukamizu, Anti-apoptotic action of angiotensin fragments to neuronal cells from angiotensinogen knock-out mice, *Neurosci. Lett.* 232 (1997) 167–170. [https://doi.org/10.1016/S0304-3940\(97\)00605-8](https://doi.org/10.1016/S0304-3940(97)00605-8).
- [18] Heidemann SR, Reynolds M, Ngo K, Lamoureux P. The culture of chick forebrain neurons. *Methods Cell Biol.* 2003;71:51-65. doi: 10.1016/s0091-679x(03)01004-5. PMID: 12884686.
- [19] A. Kumar, B.N. Mallick, Long-term primary culture of neurons taken from chick embryo brain: A model to study neural cell biology, synaptogenesis and its dynamic properties, *J. Neurosci. Methods.* 263 (2016) 123–133. <https://doi.org/10.1016/j.jneumeth.2016.02.008>.
- [20] E.J. De Genst, T. Guilliams, J. Wellens, E.M. Day, C.A. Waudby, S. Meehan, M. Dumoulin, S.T.D. Hsu, N. Cremades, K.H.G. Verschueren, E. Pardon, L. Wyns, J. Steyaert, J. Christodoulou, C.M. Dobson, Structure and properties of a complex of  $\alpha$ -synuclein and a single-domain camelid antibody, *J. Mol. Biol.* 402 (2010) 326–343. <https://doi.org/10.1016/j.jmb.2010.07.001>.
- [21] C.C. Cabalteja, S. Sachdev, R.W. Cheloha, Characterization of a Nanobody-Epitope Tag Interaction and Its Application for Receptor Engineering, *ACS Chem.*

Biol. 17 (2022) 2296–2303. <https://doi.org/10.1021/acscchembio.2c00407>.

- [22] Tsutsui, H., Jinno, Y., Tomita, A., Niino, Y., Yamada, Y., Mikoshiba, K., Miyawaki, A. and Okamura, Y. (2013), Improved detection of electrical activity with a voltage probe based on a voltage-sensing phosphatase. *The Journal of Physiology*, 591: 4427-4437. <https://doi.org/10.1113/jphysiol.2013.257048>
- [23] M. Zeghal, K. Matte, A. Venes, S. Patel, G. Laroche, S. Sarvan, M. Joshi, J.C. Rain, J.F. Couture, P.M. Giguère, Development of a V5-tag–directed nanobody and its implementation as an intracellular biosensor of GPCR signaling, *J. Biol. Chem.* 299 (2023) 105107. <https://doi.org/10.1016/j.jbc.2023.105107>.
- [24] H. Götzke, M. Kilisch, M. Martínez-Carranza, S. Sograte-Idrissi, A. Rajavel, T. Schlichthaerle, N. Engels, R. Jungmann, P. Stenmark, F. Opazo, S. Frey, The ALFA-tag is a highly versatile tool for nanobody-based bioscience applications, *Nat. Commun.* 10 (2019) 1–12. <https://doi.org/10.1038/s41467-019-12301-7>.
- [25] O. Gokce, T.C. Südhof, Membrane-tethered monomeric neurexin LNS-domain triggers synapse formation, *J. Neurosci.* 33 (2013) 14617–14628. <https://doi.org/10.1523/JNEUROSCI.1232-13.2013>.

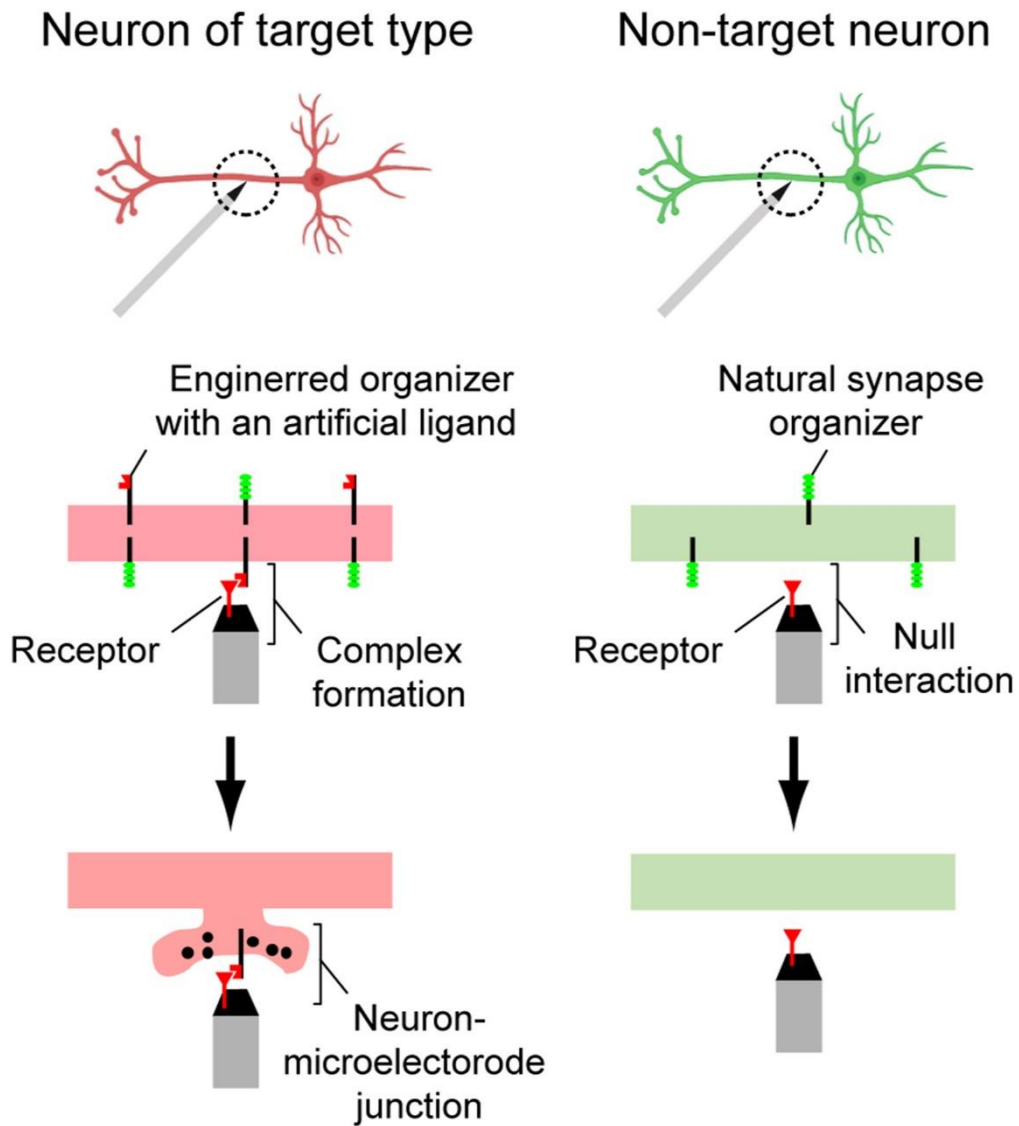


**Fig. 1** Role of an engineered synapse organizer for the formation of cell-type-specific neuron-microelectrode junction. The microelectrode functionalized with a receptor exerts synapse differentiation in contact with a target neuron expressing the engineered organizer with an artificial ligand, through the formation of the ligand-receptor complex (left) but not with a non-target neuron (right).



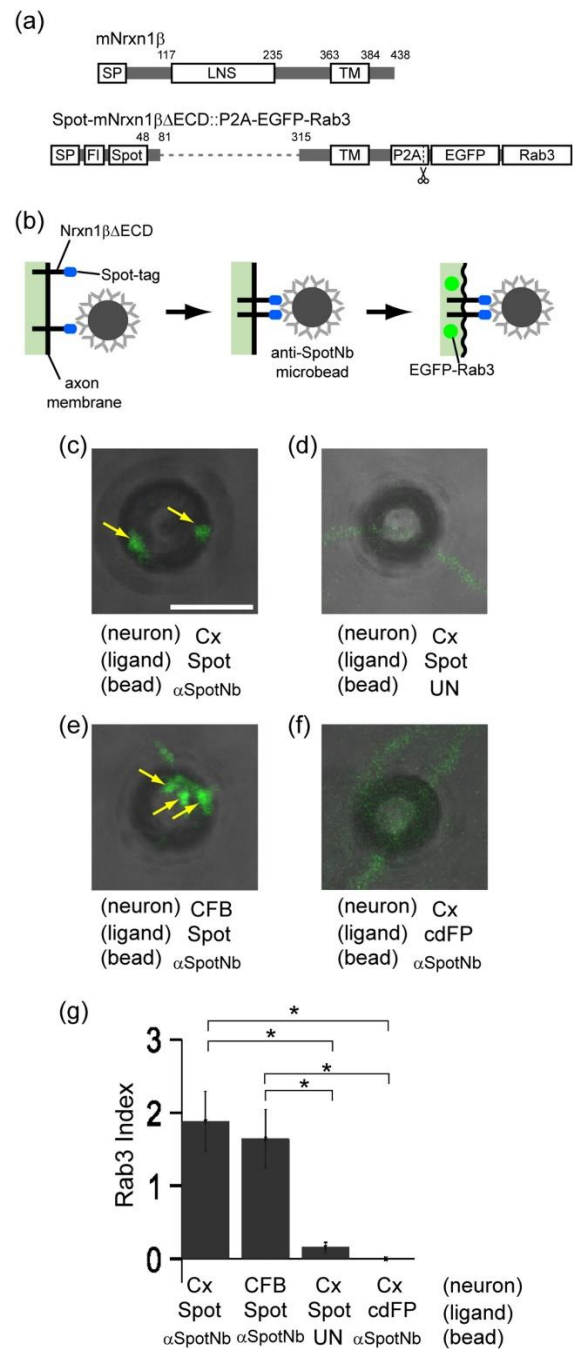


**Fig. 2** (a) A design of mNRXN-1β-based engineered organizer. (b) A scheme showing microbeads assay of the synaptogenic function of an engineered organizer. (c-f) Representative results of microbeads assay in the four conditions noted. Cx: cortical neuron, UN: undecorated, CFB: chick forebrain neuron, cdFP: chromophore deficient variant of a green fluorescence protein. Arrows indicate Rab3 accumulations. Bar = 5 μm; applied to all images. (g) Analysis of Rab3 index in four conditions indicated. Asterisks indicate significance in the Tukey test (\*p < 0.1%). The number of samples was 26, 16, 18, and 24 from left to right.

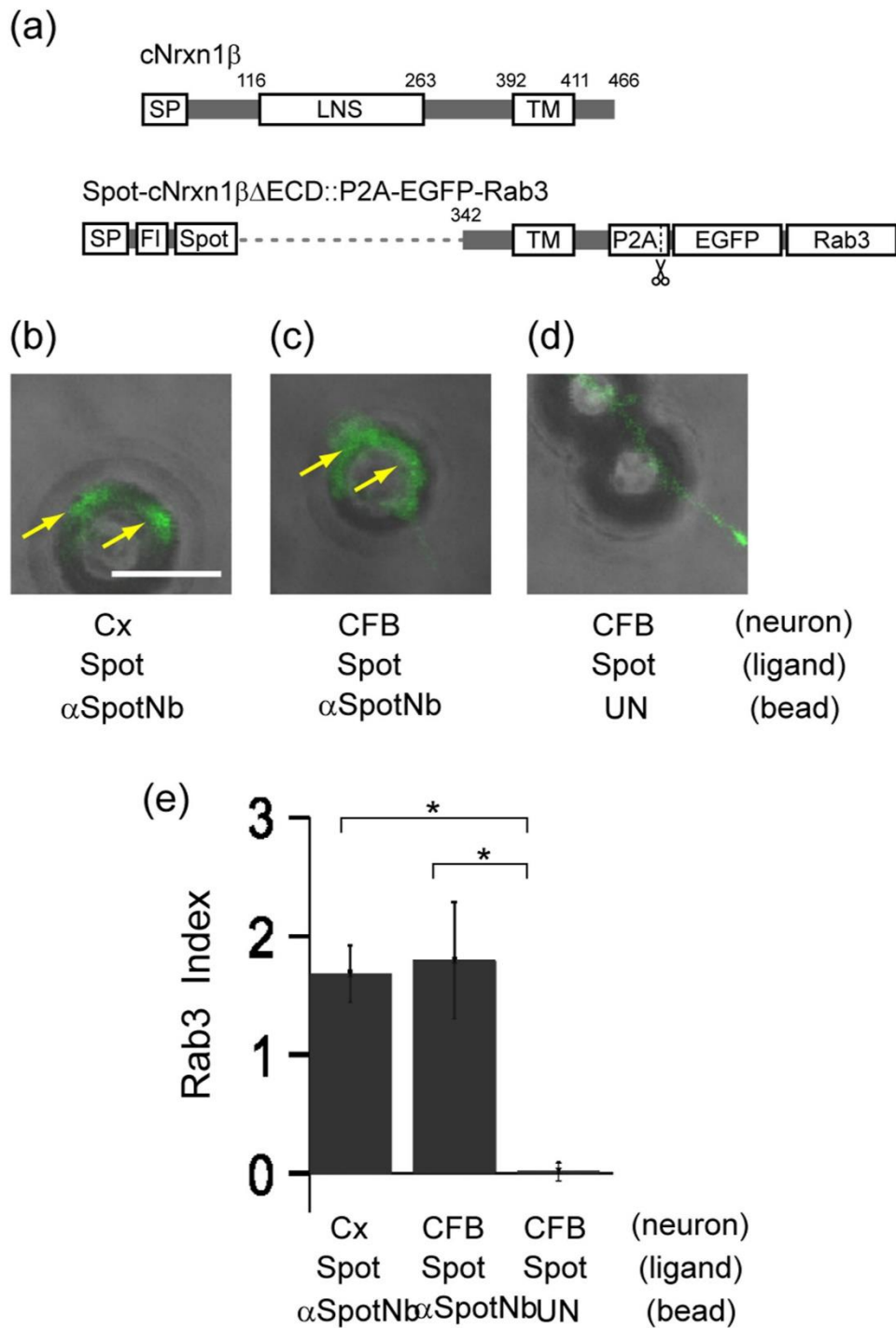


**Fig. 3** (a) A design of chick NRXN-1 $\beta$ -based engineered organizer. (b-d) Representative results of microbeads assay in the three conditions noted. Arrows indicate Ra3 accumulations. Bar = 5  $\mu$ m; applied to all images. (e) Analysis of Rab3 index in the conditions indicated. Asterisks indicate significance in the Tukey test (\* $p < 0.1\%$ ). The number of samples was 28, 14, and 13 from left to right.

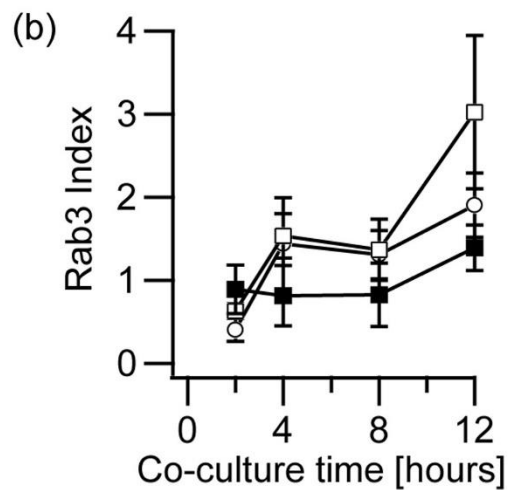
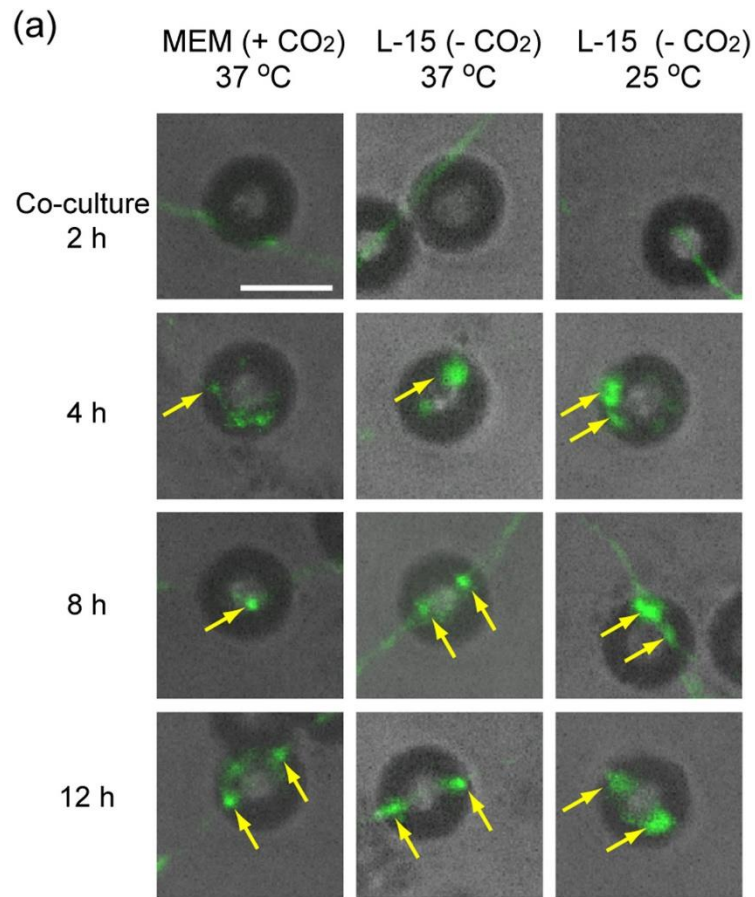


**Fig. 4** (a) Representative results of microbeads assay after co-culture of the different times as indicated. Some of the Rab3 accumulations are indicated by arrows. Bar = 5  $\mu$ m; applied to all images. (b) Rab3 index versus co-culture time plots. Data in Mem (+ CO<sub>2</sub>, 37 °C), L15 (- CO<sub>2</sub>, 37 °C), and L15 (- CO<sub>2</sub>, 25 °C) are plotted in open circle, open square, and filled square, respectively. The number of samples ranged from 11 to 25.

```

mNrxn1β      1: MYQRM LRCGADL GSPGGSSGGGAGGRLAL I WIVPLT LSGLLGVAWGASSLGAHHIHHFHG 60
cNrxn1β      1: MGGF-LRGSPEFGPAGGSSGS-AGGRLAL I WIVPLT LSGLLGVAWGASSLGAHHIHHFHG 58

mNrxn1β     61: SSKHHSVPIAIYRSPASLRGGHAGTTYIFSKGGGQITYK WPPNDRPSTRADRLAIGFSTV 120
cNrxn1β     59: SSKHHSVPIAIYRSPASLRGGHAGTTYIFSKGGGQITYK WPPNDRPSTRADRLAIGFSTV 118

mNrxn1β    121: QKEAVLVRVDSS SGLGDYLELH HQGKIGVKFN VGTDDIAIEE S NAIINDGKYHVVRFTR 180
cNrxn1β    119: QKEAVLVRVDSS SGLGDYLELH HQGKIGVKFN VGTDDIAIEE I NAIINDGKYHVVRFTR 178

mNrxn1β    181: SGGNATLQVDS WPVIERYPAG -----RQLTIFNSQ 210
cNrxn1β    179: SGGNATLQVDN WPVIERYPAG NNDNERLAIARQRI PYRLGRV VDEWLLDKG RQLTIFNSQ 238

mNrxn1β    211: ATIIIGGKEGQ PFQQLSGLYNG LKVLNMAA ENDA NIAI V GNVRLVGEVPSSMTTEST 270
cNrxn1β    239: ATIKIGGKEGSH PFQQLSGLYNG LKVLNMAA ENDA NIV I E GNVRLVGEVPSSMTTEST 298

mNrxn1β    271: ATAMQSEMSTS IMETITTLAT STARRGK EPTKEPI SQTDDILVSAECP SDDDEDIDPCE 330
cNrxn1β    299: ATAMQSEMSTS VMETITTLAT STARRGK APTKEPI GQTDDILVSAECP SDDDEDIDPCE 358

mNrxn1β    331: PSSGGLANPTR VGG-REYYPGSAE VVIRESSSTTGM VVGIVAAAAALC ILLIYYAMYK YRNR 389
cNrxn1β    359: PSSGGLANPTR AGGGR-EYYPGSAE VVIRESSSTTGM VVGIVAAAAALC ILLIYYAMYK YRNR 417

mNrxn1β    390: DEGSYHVDESR NYISNSAQSN GAVVKEKQPS SAKSANKN KKNKDKEY YV 438
cNrxn1β    418: DEGSYHVDESR NYISNSAQSN GAVVKEKQPS SAKSANKN KKNKDKEY YV 466

```

**Fig. S1** Alignment of amino acid sequences of mNRXN-1 $\beta$  (Seq. ID: NP\_001333889.1) and cNRXN-1 $\beta$  (Seq. ID: NP\_001185905.1). Identical residues are boxed. The LNS domain, transmembrane domain, and the PDZ domain binding motif are shown in blue, gray, and pink, respectively. The asterisks indicate seven mismatches in the region used in the constructs. Note that the gap after G<sub>201</sub> in the LNS domain of mNRXN-1 $\beta$  is due to ss4(-) alternative splicing and the coding amino acid sequence in that region is an exact match to cNRXN-1 $\beta$  (see Seq. ID: NM\_001346959.2).

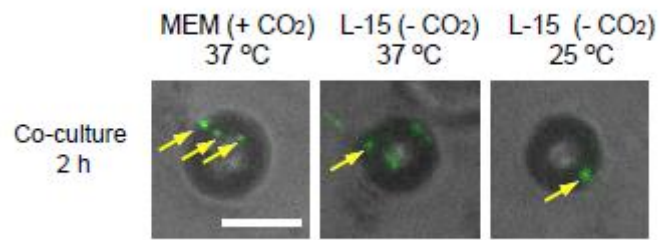


**Fig. S2** Examples of Rab3 accumulations in the microbeads assay in co -culture time of 2 hours. The arrows indicated accumulations. Bar = 5 mm; applied to all images.

## Chapter 3

# Development of Glass Microelectrodes with the Ability to Induce Synapse Formation

### Purpose of Chapter 3

- Establish a method for fabricating glass microelectrodes with synapse organizer molecules immobilized on the tip.
- Establish a method for immobilizing synapse organizer molecules on glass microelectrodes and confirm how they are immobilized.

### Achievement

- A simple method for fabricating glass microelectrodes was established using the electrode fabrication equipment used in the patch-clamp method.
- The protein was effectively immobilized by applying a pulse voltage to the metal part at the tip of the electrode in a protein solution. Fluorescent proteins were indirectly immobilized, and the immobilization was confirmed by observing the fluorescence.

### Remaining Challenges

- Circuit design and electrode shape optimization for measurement via glass microelectrodes.

### Chapter 3 Key Points

- Proteins were immobilized by applying a rectangular pulse voltage to the gold surface at the tip of a glass microelectrode.
- Using a micropipette puller and FIB (Focused Ion Beam), gold was successfully exposed at the tip of a glass microelectrode.
- A protein called ProteinA was bound to the tip of the fabricated glass microelectrode to allow binding of proteins with optional Fc regions.
- Protein immobilization experiments using the fabricated glass microelectrodes suggest that the voltage value of the rectangular pulse and the period of the pulse are important.
- The mechanism of protein immobilization and a highly reproducible micropipette puller processing method remained unresolved.



## Introduction

As described in Chapter 2, I performed co-culture of microbeads and Chick, Rat neuron transfected with epitope-tagged NRXN-1 $\beta$ , which was developed based on NRXN-1 $\beta$  from mammals and birds, and observed its activity. By combining Anti BC2 Nanobody and SPOT-tag added to the N-terminus of NRXN-1 $\beta$ , I was able to induce synaptogenesis by promoting the clustering of NRXN-1 $\beta$ . Based on this result, I considered that applying this mechanism to the tip of a glass microelectrode such as used in the patch clamp method, it would be possible to make synapses between the electrode tip where Anti BC2 Nanobody was immobilized and the fabricated Axon of neuron transfected with NRXN-1 $\beta$ . In Chapter 2, binding by Anti BC2 Nanobody and SPOT-tag induces synaptogenesis by clustering NRXN-1 $\beta$  at the presynaptic terminal, but I am interested in performing selective neuronal observation by using different peptide tags.

The patch clamp technique is an electrophysiological technique that can directly measure the membrane potential and the amount of current flowing across the plasma membrane. It was developed by Erwin Neher and Bert Sakmann, who was awarded the Nobel Prize in Physiology or Medicine for achieving single-channel recording in 1991 [1]. The patch clamp technique is an electrophysiological technique that can directly measure the membrane potential and the amount of current flowing across the plasma membrane.

Since the patch clamp technique was first developed, various derived techniques have been actively developed to this day [2,3,4]. However, this technique also has a problem that a specific cell cannot be selectively observed. Based on the experience I have gained so far; I have been able to create a glass microelectrode by an original technique. By placing the fabricated electrode tip and a silver chloride electrode in a protein solution and applying a pulsed voltage, the protein in the solution is immobilized on the gold surface at the tip of the electrode. By this technique, synapse organizer molecules were immobilized on the electrode tip. Although many have proposed that protein adsorption on the surface is linked to factors such as the zeta potential and the isoelectric point, there is still no theory that can provide a unified explanation [5, 6, 7, 8]. There are also studies that have shown that it is possible to immobilize proteins on electrodes using a direct current voltage or a pulsed voltage [9, 10, 11].

In order to realize selective cell observation, I developed a prototype microelectrode for next-generation neural activity recording with cell recognition function using synaptic organizer molecules that induce synapses.

## **Materials and Methods**

In order to make a glass micropipette-type microelectrode with cell-selectivity compatible with conventional patch-clamp instruments, I designed its overall shape, including the

back of the electrodes and the lengths of the tubes, so that it was no different from the glass electrodes used for patch-clamp applications. This allowed us to make connections to manipulators and ensure conduction without any problems. The fabrication method of the electrodes was based on the work of B. B. Katemann and W. Schuhmann[12]. Platinum-containing microelectrodes and their development method are presented [1]. In this study, I used borosilicate glass tubes and gold wires to make glass microelectrodes. The glass microelectrode fabrication method is described separately for each item below.

### **Seal**

I made a SEAL MACHINE (**Fig. 1a**). I used a Cantal wire heater (PC-10H, NARISHIGE) as the filament. I vacuumed the glass tube from the left and right sides using a vacuum pump (DAP-6D, ULVAC KIKO) while heating the glass tube with a gold wire (NILACO, 0.08 [mm]) of about 1 [cm] at the center filament, so that the glass at the filament position was shrunk and sealed (**Fig. 1b**). The ultimate pressure of the vacuum pump I used was 6.65 [kPa]. The heating time by the filament was 2 minutes and 20 seconds, and the current and voltage values were set at 12.20 to 13.20 [A] and 3 to 4 [V], respectively. I performed sealing while observing the gold wire shrinking surrounded by the molten glass using an optical microscope. I adjusted the voltage and heating time accordingly. I made a straight gold-sealed glass.

## **Pull**

A metal wire was inserted inside a glass tube, sealed, and pulled simultaneously with a micropipette puller (P-1000, SUTTER INSTRUMENT). The metal wire was stretched thin (as in Kintaroame), while leaving room for glass and gold for later processing. A glass micropipette containing gold immediately after pulling (**Fig. 1c**). The P-1000 can be programmed to adjust the pulling of the glass tube, and a typical glass pipette for patch clamping can be made with good reproducibility by using the filaments and programs listed in the recipe book. The programs and filaments for making the microglass tube electrode used in this process are shown in Table 1. The Ramp test was always executed before the experiment to confirm the parameters such as Ramp value, temperature, and humidity before pulling. For the first pull of the experiment day, carefully check [View Pull Results] in the Menu of the Program. Program adjustment is done mainly by changing the Heat parameter; changes in Pull and Vel other than Heat have been found to have a significant effect on electrode shape. By carefully checking the [View Pull Results] and making adjustments to get close to the last successful [View Pull Results], such as slightly increasing the Heat if the Ramp value is low or slightly decreasing the Heat if the temperature is high, it is possible to efficiently fabricate an electrode with a good shape

in which the gold is fully connected inside the glass capillary.

The prepared electrode is examined with an optical microscope near the glass tip, and if the gold is conductive from the inside of the glass tube to the tip, the tip is processed in the next step.

### **FIB Processing**

Once the gold-filled glass pipette is prepared, it is processed by a focused ion beam machine (SMI-3050, Hitachi High-Tech Science Corporation). The focused ion beam machine (FIB) is a machine that processes a sample by focusing an ion beam and irradiating it with the focused ion beam. The resolution is 30 kV and 4 nm, and the tip diameter of the glass microelectrode to be processed this time is 1 to 5 [ $\mu\text{m}$ ] (**Fig. 1d**). Since the gold at the electrode tip cannot be seen during processing unless the gold is grounded, the FIB machine placed the electrode on a special pedestal and grounded the gold inside the electrode securely. The tip was processed by cutting it with a beam etching function. The goal was to process the electrode tip into a pencil shape with a sharp point. By making four cuts at different angles, I finished it into a square pyramid shape. I adjusted it so that the gold was exposed at the apex. This shape was devised to immobilize the synapse organizer molecules only at the electrode tip, and the tip diameter of 1 to 5

[ $\mu\text{m}$ ] should be similar to the particle size of the microbeads used in Chapter 2.

### **Protein Immobilization**

An antibody-binding protein, ProteinA (TCI chemicals, Tokyo, Japan), was immobilized on the tip of FIB-processed glass microelectrodes using a technique unique to our laboratory and described in the introduction (**Fig. 1e**). I used this "Protein Labeling" to immobilize ProteinA on the electrode tip and further bound proteins that bind ProteinA, such as Fc Venus (a fluorescent protein) and Fc BC2 Nanobody (a nanobody that binds to epitope-tagged NRXN-1 $\beta$  created in this study). I unbound the Fc region by washing with MgCl<sub>2</sub> and switched the protein to be immobilized on the surface of the electrode with ProteinA.

The protein solution used in the protein immobilization experiments was made from a buffer containing ProteinA. The buffer was 20 mM Hepes (pH 9.0) + 0.05% TritonX mixed with 5 mM NaCl. 400 [ $\mu\text{l}$ ] of the buffer was prepared, and 2 [ $\mu\text{l}$ ] of ProteinA was used in the experiments. Triton-X contained in the buffer was a surfactant and was used to avoid immobilization of unnecessary proteins on the glass surface of the electrode. A disk-shaped silicon chamber (outer diameter 1.2 [cm], inner diameter 0.5 [cm], thickness 1 [mm]) was attached to a slide glass with PDMS, and 50 [ $\mu\text{l}$ ] of ProteinA solution was

placed. A silver chloride electrode and a glass microelectrode were placed in the ProteinA solution, and a pulse voltage was applied between the microelectrode and silver chloride using a source meter (2401, Keithley). A pulse voltage was applied by connecting to the source meter via a breadboard so that the current value could be monitored by the source meter. The electrode was fixed with a patch clamp manipulator (U-1C, NARISIGE) and the silver chloride electrode was fixed with a negative electrode. The glass microelectrode was fixed to a pipette holder and then set on the manipulator. The silver chloride electrode was fixed to a rod (H-1, NARISIGE) and then set. The pulse voltage was set between 1.7 - 2.4 [V], and the width of a rectangular pulse was set between 50 or 100 [ms]. The magnitude of the voltage was determined by checking the diameter of the electrode tip and how much current flowed in a test just before the experiment. The number of pulses was set to be between 100 or 200 times as 1 set, and the voltage and the number of pulses were adjusted accordingly while observing the current waveform. The most typical pattern was 2.0 [V], 50 [ms]  $\times$  200 pulses, 2 sets.

After the application of the pulse, the electrode was washed with pure water and overnight in the optional Fc protein. After the overnight, the electrode was removed and washed with PBS (phosphate-buffered saline) before observation, experiment, etc. Since the electrode can be washed and reused as long as it is not destroyed, the electrode with

immobilized ProteinA was stored in PBS as much as possible, and when the immobilization of ProteinA was performed again, all organic matters on the electrode tip were removed with Piranha solution, and then the experiment was repeated.

## **Microscopy**

When Fc Venus was bound to the tip of the electrode, the presence of ProteinA can be indirectly confirmed by fluorescence observation because the binding between Fc protein and ProteinA is almost certain. Fluorescence observation was performed with a microscope (IX71, Olympus) connected with a xenon lamp (Ushio, Tokyo) and a CCD camera (Orca Flash 4.0 C11440, HAMAMATSU). Excitation filters from 460 to 480, emission filters from 495 to 540 (Olympus), and a 490 GFP dichroic mirror were used to observe Fc Venus. Data were acquired using IDL (Research Systems, USA) and analyzed with ImageJ.

## **Results**

The results of the protein-immobilization experiments, showing the fluorescence of the tip of the electrodes (**Fig. 2, 3**). I used a low voltage in Figure 2 and a high voltage in Figure 3. The ProteinA solutions used were all of the same composition and were



previously described in the section on Protein Immobilization. The results of the experiments showed that ProteinA could be immobilized on the tip of the electrodes when pulsed voltage was applied to the electrodes in ProteinA solutions to make Fc-Venus overnight. I used piranha solutions to remove ProteinA. Piranha solutions are strong organic solvents made by mixing concentrated sulfuric acid with hydrogen peroxide in a ratio of 3:1. Because of the risk of explosion, I had to make sure that concentrated sulfuric acid was placed in the vessel first and hydrogen peroxide was mixed in it. I made piranha solutions and immediately put the tip of the electrodes in it and washed them. I could confirm the removal of organic matter by confirming the generation of bubbles, so I washed them until no bubbles were generated. After washing, I performed fluorescence observation again and confirmed that no fluorescent proteins were observed, so I found that both electrodes could be washed in about 10-15 seconds. Also, as previously described, I could only release Fc binding with MgCl<sub>2</sub> solutions. I prepared MgCl<sub>2</sub> solutions, washed the tip of the electrodes for about 10 seconds, and observed under a microscope that no fluorescence remained. Then, I could overnight with any Fc proteins (FcBC2 Nanobody, in this study) and switched the proteins immobilized on the tip of the electrodes.

By observing the fluorescence of Fc Venus and indirectly confirming the immobilization

of ProteinA, it can be said that Fc BC2 Nanobody could be immobilized in a similar manner. The diameter of the electrode tip was almost the same as the microbeads used in the experiments in Chapter 2, and the situation in which Fc BC2 Nanobody is immobilized by Fc-binding in it can also be said to be the same. Therefore, it is expected that the results of the experiments on inducing synaptogenesis in microbeads in Chapter 2 can be obtained by bringing the glass microelectrode prepared here into contact with Neuron.

### **Notes on Experiments**

The rough flow of the experiment has already been explained in Materials and Methods, but the knowledge obtained by actually preparing the electrode is shared below. The precautions in the preparation of the glass microelectrode are explained item-by-item below.

### **Seal**

The transition temperature of borosilicate glass is 525 °C, and the filament is heated to approximate this temperature. At this temperature, the gold does not change and is only enclosed and enclosed in the glass. To prevent static electricity from causing the thin gold

to stick to the glass, rubber gloves are not worn when gold is placed in the glass tube. By picking up the gold at the end of the glass tube, the gold can be placed in the glass tube without bending the gold line. It has been found that stretching the gold as much as possible does not adversely affect the subsequent pull, so the bent gold is used as much as possible. It can be straightened by rolling the gold, but it is difficult to remove the strain once it has been applied to other than 0.08 [mm], for example, 0.10 [mm], and it is difficult to handle 0.05 [mm] for the same reason. Since the change in the diameter of the gold line also requires adjustments in the program used for the subsequent pull, the processing is performed under unified conditions if possible. Although it is not an essential element, it is important for the subsequent pull process that neither the glass tube nor the gold is subjected to excessive force as much as possible, and the change is minimized.

The sealing machine consists of a heating mechanism by a filament and a glass tube fixing part as shown in Figure 1a. The heating mechanism is made by cutting an aluminum rod and carving a screw hole and a groove to guide the filament. The glass tube fixing part is also made by carving a screw hole and a groove, and the same four aluminum parts are used in total. It is good if the temperature at which the filament can output is high enough to melt the electrode. However, if the current value is too high or the glass tube is in

contact with the filament, the glass tube will melt away. It is carefully observed under the microscope for changes in the glass through the filament. When the preparation of the device is completed, before heating the glass tube, a vacuum pump is connected to both sides of the electrode by a tube and air is pulled. After sealing, the encapsulation of the electrode is confirmed by attaching a silicon tube of about 1.0 [mm] to the disposable syringe and connecting it to the sealed glass tube. If the electrode is encapsulated around the center, it can be confirmed immediately because the syringe tries to return to its original position. To prevent the influence of environmental changes, a certain number of them are sealed together and used for Pull.

## **Pull**

It was processed using a micropipette puller (P-1000, SUTTER). At present, I use the program shown in Table1, but it is highly dependent on the state of the filament. In addition, I have confirmed that changes in temperature and humidity affect the Pull result. Therefore, I clarify here that basically the same program does not guarantee the same result. During the search for a suitable program, I changed the type of filament and the program to match it, and finally I was able to create a glass electrode in which the gold was continuous inside.

As already mentioned, the parameter adjustment is mainly carried out by changing only the Heat. The guideline for the Heat parameter is the Ramp value + 10. Pull and Vel are greatly related to the shape of the electrode, and frequent changes in the electrode shape are not desirable in this study in which the state of the electrode tip is important. In order to stabilize the experimental results, the Ramp value was measured after the start of the experiment, and the program was run as it was if the value, room temperature, and humidity did not change greatly from the previous experiment. If there was a change in the Ramp value, the Heat was adjusted accordingly. The Ramp value in significant environmental changes, such as the Ramp value in summer and winter, changed greatly, but the Ramp value usually did not change greatly to 10 or 20 in a month. If there was a change, the change or breakage of the filament and the state of the machine had to be checked and adjusted again. For the reasons mentioned above, it was important to keep the room temperature constant, so in this experiment, the experiment was carried out by fixing the room temperature to 23-24 °C. The humidity varied from 30% to 70%, but if the humidity was higher than 50%, the Heat was also adjusted up, and on the contrary, if the humidity was lower than 50%, the Heat was adjusted down. The adjustment range of the Heat was basically 5. The most important thing in the Pull is the adjustment of the program, and it is the key to finish the adjustment early on the day of the experiment.

When the adjustment of the program is successful and the electrode with a good shape is completed, as many electrodes as possible are pulled and stocked. When the experiment is carried out on an annual basis, it is convenient to record the good programs roughly by seasons.

After completion of Pull, the electrodes were stored on a plastic Petri dish with thick double-sided tape placed on it.

### **FIB Processing**

Various preparations are required before FIB processing. In particular, it is important to protect both the equipment and electrodes when using the FIB equipment. Since the main chamber where the FIB equipment is processed must be kept in a vacuum state, the electrodes, and the FIB stage where the electrodes are installed must be cleaned in advance to eliminate organic contamination. A pointed contact probe (C-NP20, MISUMI) was packed into the electrode to ensure the electrical connection of the electrode.

In some electrodes, the gold is not exposed at the tip. In that case, the glass tube is removed until the gold is exposed and prepared for FIB processing. A small scissor or tweezers is used for processing. The glass at the tip of the electrode is in the form of a string, and that portion is cut off and the gold is connected to the tip of the glass tube.

When protein immobilization experiments are performed, attention is paid to the crack of

the glass because proteins may enter the inside of the glass tube through the crack of the glass. Such pre-processing of the tip shape is only an aid for FIB processing, and it is not for re-processing a relatively thick electrode or a destroyed electrode to finish it into a thin electrode by FIB processing. It is performed only when it is necessary as spare processing. It is difficult to reuse an electrode that failed in Pull (thick tip, gold is not connected inside, etc.).

A special stage was fabricated for FIB processing (**Fig. 4a**). A conductive tape was used to secure the electrode to the stage, and a contact probe (CP) was inserted inside. The CP was pressed from the inside to the tip of the electrode to measure the conduction (**Fig. 4b**). It was confirmed microscopically that the gold was touching the CP. Since the CP alone was not long enough to protrude outside the glass tube, a metal wire (0.40 [mm], brass, Dydo Hunt) of about 1 [cm] was pressed from the back of the CP to push in the CP, and the metal wire was pressed and fixed by a metal plate. Since the CP was fixed while being pressed by the metal wire, the CP was always in a pressed state, which was an indicator of good electrical conduction.

Next, I explain machining with the FIB device. As previously described, the FIB device is used to sharpen the tips of the electrodes in a pencil-like shape, and the electrodes are shaved with a laser so that the gold is exposed. The following detailed explanation is

based on the FIB device SMI-3050. The electrodes installed in the FIB device are oriented so that the tips of the electrodes are oriented in the downward direction ( $180^\circ$ ) on the Stage Controller screen of the FIB. During FIB operation, the tips of the electrodes can be oriented upward on the screen by setting the Scan Rotation to  $180^\circ$  in advance. This makes it easier to see when the electrodes are tilted. The stage is attached to the holder specified for the FIB device with conductive tape. It is attached to the rod and the stage is transferred to the Main Chamber. After the prescribed Daily Adjust, the process moves to the machining screen. The flow of machining (**Fig. 4**). Eucentric the electrodes with an Image Scale of  $40\text{ }\mu\text{m}$  or finer. The height (Z) after the Eucentric is recorded, and the height can be set without Eucentric again by using it after the Stage Rotation. Note that the Eucentric is required every time the Image Scale is changed. After the Eucentric, the electrodes are machined by adjusting the Scan Rotation to an arbitrary angle, mainly at an oblique angle (the image is adjusted at an oblique angle instead of the machining frame at an oblique angle). The machining frame is created after the image is captured with the Scan Speed set to 2, and the Beam type is set to URough (Rough is recommended for careful machining) and the material is set to SiO<sub>2</sub> by opening the properties of the machining frame. First, the tips are cut horizontally little by little to identify the position of the gold on the tips of the electrodes. If the gold is already visible before machining,



this machining is not necessary. Once the gold is identified, the electrodes are cut on the left and right sides at an arbitrary angle. After the cutting is completed twice, tilt is performed, and the gold is confirmed to be on the "ridge" created on the tips of the electrodes. The machining is adjusted by repeating machining a little, if necessary, but every time the machining is repeated, the electrodes become thicker, so I try to minimize the machining. After the left and right sides of the electrodes are cut, the electrodes are rotated by 90 ° in the Stage rotation (if the Scan rotation is also set to 90 °, the Scan rotation before the Stage Rotation is the same as that at 180 °). The tips of the electrodes are projected on the screen and tilted (50 ° - 60 °. For SMI-3050, the upper limit is 60 °). After tilting, the same as before. If the tip of the electrodes is less than 5 [μm], the Image Scale should be smaller than [μm] and the Rough beam should be used. In order to prevent unnecessary irradiation of the beam during machining, the machining frame during machining should be observed and the machining should be stopped by STOP when the machining is finished. The position and location of the machining frame can also be adjusted in the ST postoperative direction. If the electrodes can be formed into the target shape, the next step is taken.

## **Protein Immobilization**

The protein is immobilized on the gold exposed at the tip of the fabricated glass tube microelectrode. In order to apply the pulsed voltage, conduction is ensured by CP as in the preparation for FIB processing. Using a glass micropipette holder, the positions of the microelectrode and the silver chloride electrode were fixed, and the aforementioned protein solution was placed in a silicon chamber. I have already described the method of the experiment, so I will omit it. The experimental results show that it is possible to estimate to some extent whether the immobilization of the protein is successful by looking at the current flow during the experiment. Specifically, the probability of immobilization is high when the current waveform falls like a function with the inverse of a natural number (**Fig. 3**). In particular, the success rate of immobilization increased when the voltage value was adjusted so that the spike immediately after the pulsed voltage was applied was 0.1 [ $\mu\text{A}$ ] or more. The number of pulsed voltage applications is set to 2 sets as already described, but in the case of most electrodes, it was found that the current value decreases with each repetition of the set of pulsed voltage. In this case, the immobilization probability increases more by repeating the application of pulsed voltage until the current value becomes about 1/10. However, I cannot deny from our experience that too high voltage application and excessive number of experiments do not increase the immobilization probability.

I describe how to perform overnight after the experiment. I used a 96-well microplate for overnight. I placed approximately 200 [ $\mu$ l] of an arbitrary Fc protein solution in the well plate, and then placed the electrode tip in the well. I used a rubber band and a wooden board with a groove so that the electrode tip could be fixed in the Fc protein solution while protecting it. The wooden board was carved with a groove of about 1 [mm] at the position where the outer circumference and the electrode were fixed. The electrode was fixed along the outer circumference of the wooden board with the rubber band, and a screw was attached to prevent the wooden board from moving from the well plate (**Fig. 5**). Wet tissues for moisture retention and the well plate were placed in an airtight container and overnight at 4 °C.

### **Alternative Methods**

So far, I have described the electrode fabrication process that I mainly use at present. If I can switch methods and make appropriate electrodes according to the purpose and situation, I will be able to easily consider new electrodes using these electrodes and combinations with unprecedented methods. To create the possibility of efficiently solving future problems, I will describe different methods that I established in the past.

## **Seal**

In the past, I established a method to establish electrode conduction by spot-welding a gold wire and a stainless-steel wire. This method differs from the current method of processing with contact probes in that a dedicated terminal needs to be connected to bring the conduction to the outside of the glass tube. Therefore, I need to think about which conduction method to use the electrode before sealing it. I spot-weld a 0.10 [mm] stainless steel wire (NILACO) and a gold wire with a spot-welding machine (KTH-MWST, Kondo Tech). I cut the stainless-steel wire to a length of about 10 [cm], cross the gold and the stainless-steel wire, and spot-weld them. I place them in the glass tube, place the gold in the center, and seal them while vacuuming. I spot-weld the stainless-steel wire and the gold in only one place, but I can also do it in two places by sandwiching the gold. In that case, the two glass tubes created later by Pull may both be processed as microelectrodes if the gold is connected inside.

## **Pull**

As already mentioned, the production of glass pipettes by micropipette pullers is not stable and requires a lot of adjustments due to the continuity of the gold inside the tube.

For reference, the program used in the past is shown in Table 2.

I describe the processing of spot-welding stainless steel wire and gold. A terminal was attached to the back end of a glass tube electrode to ensure continuity for use in FIB processing and later protein immobilization experiments. A single-row IC socket (XR2C0008A, OMRON) was used. The terminal was separated into one terminal each. The terminal was of a standard that can be inserted into itself, and the terminal at the back end of the electrode and the terminal for ensuring continuity to be bonded to it were the same. All of the resin on the exterior of the IC socket was removed. The pin portion of the terminal was ground small so that it could be inserted into the glass tube. A microgrinder (UC100, URAWA) was used to polish the metal portion. After the pin was polished small, a small amount of solder was applied in advance. The back portion was cut to adjust the length so that the glass pipette could be placed on the FIB stage. The stainless-steel wire inside the glass tube was exposed when the glass tube was shortened, so it was removed leaving only 2-3 [mm] from the back end of the tube. The prepared terminal was inserted into the back end of the electrode while carefully securing the glass tube with a tool clipper or double-sided tape, taking care not to break the glass tip. The side of the terminal and the stainless-steel wire were soldered. The direction of the terminal was made as parallel as possible to the direction of the glass tube, so that the holder and the electrode could be made parallel during the experiment. After the terminal

was soldered, the stainless-steel wire and the terminal were reinforced with epoxy resin, etc. If the terminal was ready to be connected with the terminal for continuity, it could be used for FIB and experiments. The terminal for continuity could be used for spot welding and experiments by soldering it to a covered wire, etc. and connecting it to the terminal at the back end of the electrode. This method is easy to ensure continuity and can be used without repair in most cases. Continuity by CP cannot be broken when the CP pushed inside can no longer make contact with the gold, but processes such as spot welding and soldering are easy to check because of strong bonding. Two of the disadvantages are the high processing difficulty and the lack of flexibility in the processing method. It is difficult to attach the terminal so as not to break the tip of a pulled glass pipette, and the glass electrode after spot welding and attaching the terminal portion cannot be further processed unless part of it is broken. In particular, the rear portion of the glass electrode is a terminal portion, which makes it impossible to attach it to a patch clamp manipulator. This was the biggest reason for not choosing this continuity method in our experiments.

I next describe the use of gallium to ensure conduction. When gallium, indium, and tin are mixed at a ratio of 68.5%, 21.5%, and 10.0% while heating (at approximately 40 °C), gallium is converted to Galinstan™, a room-temperature liquid metal (this alloy is hereafter referred to as gallium). Gallium in liquid form is injected into the inside of the

electrode to ensure conduction. A heated and stretched disposable syringe was used to inject gallium. This method is superior to other methods in the ease of conduction, and it can also be used for protein immobilization experiments by simply attaching it to the pipette holder. The major drawbacks are the extremely high wettability of the glass and the adhesion of gallium to other devices. Even if gallium is injected into the inside of the glass tube using a syringe, if it is not injected near the gold near the tip, it will touch the glass first. Once it touches the glass, it will continue to spread through the glass wall and hardly touch the gold. It was difficult to remove gallium, and in particular, the connection with the pipette holder was noticeably contaminated and damaged by gallium. Although it is characterized by the ability to ensure the conduction of the glass microelectrode later, it was difficult to handle due to the liquid.

### **Protein Immobilization**

Streptavidin-Alexa 488 (Thermo Fisher Scientific, USA) or ProteinA-Alexa could be immobilized on the electrode tip in the same way as the immobilization of ProteinA. However, these proteins had weaker fluorescence than ProteinA and were more easily immobilized on the glass part. The advantage of immobilizing these proteins on the electrode tip is that the fluorescence can be observed directly without Fc Venus overnight.

Although they may be useful when searching for protein immobilization conditions, since different proteins are expected to have different optimal immobilization conditions, these proteins were not used in this experiment because I aimed to produce a microelectrode, which was the original purpose.

## **Discussion**

In this chapter, I recorded in detail the technique that realized the immobilization of proteins on the gold surfaces at the tips of the developed glass microelectrodes. The fabrication method of the electrodes was based on the conventional patch-clamp method and the technique developed by B. B. Katemann et al. [12]. Although I was able to immobilize ProteinA on the tip of the fabricated microglass tube electrode, the mechanism of protein adsorption, which is the core of this technology, is not deeply understood. There is an opinion that two large forces, ionic amine-silanol bond and cooperative aggregation force between protein and glass, are involved in protein adsorption. Usually, proteins are adsorbed more easily on the glass surface, but our experimental results show that they are rather adsorbed more strongly on the gold tip than on the glass. Although pH is considered to be an important factor related to protein adsorption, it is also suggested that the state of water as a medium has a greater effect [8,



9, 13, 14]. However, in this study, when the electrode tip was immersed in the protein solution, almost no active immobilization of proteins on the glass part was observed in a wide area near the tip, which is probably because the number of proteins immobilized on the gold surface of the electrode tip was larger than that of proteins (ProteinA, Fc Proteins) that might have adhered to the glass. Although I did not attempt to change the pH or immobilize proteins other than ProteinA in the present experiments, it is possible that induction by electrical force, as suggested by many literatures [11, 16, 20], acted on the proteins to immobilize them efficiently on the tip of the electrode area.

Protein adsorption on the metal surfaces was effectively performed using a pulsed voltage. Comparing the results of Figure 2 and Figure 3, it is considered that the voltage of about 2.0 [V], the pulse width of 50 [ms], and the number of times of 200 are more likely to immobilize the protein more efficiently. Since the results of the experiments with dc voltage are not available, it is not clear which is easier to immobilize the protein compared with pulsed voltage. However, the experiments performed with dc, ac, and pulsed voltages all confirmed the immobilization of the protein [6, 10, 19], so the method of this experiment is considered to be sufficiently reproducible for the experiment, while the more efficient method remains unknown. Additionally, some studies suggest that the immobilization of proteins on electrodes is related to the magnitude of the external

electric field, and at least the results of this experiment are not inconsistent with them [5, 10]. In order to establish an efficient protein immobilization method and to prevent unnecessary protein immobilization on the electrode, clarification of such protein adsorption phenomena is a future issue. Once protein adsorption technology is established, it is expected to become a technology that spans both the biological and physical fields, and it is expected to be the basis of various new technologies. In addition, protein desorption phenomena on metal surfaces are also expected to be elucidated. For implant devices with metal-based or glass surfaces that operate in vivo, protein adsorption must be controlled [14, 17, 18]. Elucidation of the mechanism of protein adsorption and desorption will be important for such areas as well. Elucidation of the mechanism will require real time observation of adsorption phenomena, detailed analysis of adsorption surfaces, and combinations of different types of metals and proteins.

I am interested in selective neuronal observation and elucidation of the mechanism of protein adsorption on metals by fabricated electrodes. The former allows evaluation of the performance of glass microelectrodes by making contact with Neuron and acquiring data as in the patch clamp method, while the latter considers it important to expand the knowledge on protein adsorption and acquire and analyze quantitative data.

## References

- [1] NEHER, E., SAKMANN, B. Single-channel currents recorded from membrane of denervated frog muscle fibres. *Nature* **260**, 799–802 (1976).
- [2] Hamill, O P et al: Improved patch-clamp techniques for high-resolution current recording from cells and cell-free membrane patches. *Pflugers Archiv : European journal of physiology* vol. 391,2 (1981): 85-100. doi:10.1007/BF00656997
- [3] Kodandaramaiah SB, Franzesi GT, Chow BY, Boyden ES, Forest CR (2012): Automated whole-cell patch-clamp electrophysiology of neurons in vivo. *Nat Methods* 9: 585–587.
- [4] Schroeder K, Neagle B, Trezise DJ, Worley J (2003): IonWorks™ HT: A new high-throughput electrophysiology measurement platform. *J Biomol Screen* 8: 50–64.
- [5] Htwe EE, Nakama Y, Yamamoto Y, Tanaka H, Imanaka H, Ishida N, Imamura K (2018): Adsorption characteristics of various proteins on a metal surface in the presence of an external electric potential. *Colloids Surf B Biointerfaces* 166: 262–268.
- [6] Wang Z, Yan Y, Qiao L (2017): Protein adsorption on implant metals with various deformed surfaces. *Colloids Surf B Biointerfaces* 156: 62–70.

- [7] Lapizco-Encinas BH, Ozuna-Chacón S, Rito-Palomares M (2008): Protein manipulation with insulator-based dielectrophoresis and direct current electric fields. *J Chromatogr A* 1206: 45–51.
- [8] M. Rabe, D. Verdes, S. Seeger, Understanding protein adsorption phenomena at solid surfaces, *Adv. Colloid Interface Sci.* 162 (2011) 87–106.  
<https://doi.org/10.1016/j.cis.2010.12.007>.
- [9] [1] H. Noh, S.T. Yohe, E.A. Vogler, Volumetric interpretation of protein adsorption: Ion-exchange adsorbent capacity, protein pI, and interaction energetics, *Biomaterials.* 29 (2008) 2033–2048.  
<https://doi.org/10.1016/j.biomaterials.2008.01.017>.
- [10] J. Barberi, S. Spriano, Titanium and protein adsorption: An overview of mechanisms and effects of surface features, *Materials (Basel).* 14 (2021).  
<https://doi.org/10.3390/ma14071590>.
- [11] S. Takahashi, K. Kishi, R. Hiraga, K. Hayashi, Y. Mamada, M. Oshige, S. Katsura, A new method for immobilization of his-tagged proteins with the application of low-frequency AC electric field, *Sensors (Switzerland).* 18 (2018).  
<https://doi.org/10.3390/s18030784>.
- [12] B.B. Katemann, W. Schuhmann, Fabrication and characterization of needle-type Pt-

disk nanoelectrodes, *Electroanalysis*. 14 (2002) 22–28.

[https://doi.org/10.1002/1521-4109\(200201\)14:1<22::AID-ELAN22>3.0.CO;2-F](https://doi.org/10.1002/1521-4109(200201)14:1<22::AID-ELAN22>3.0.CO;2-F).

[13] Suvajyoti Guha, Joshua R. Wayment, Mingdong Li, Michael J. Tarlov, and Michael

R. Zachariah Langmuir, Characterizing the Adsorption of Proteins on Glass

Capillary Surfaces Using Electrospray-Differential Mobility Analysis 2011 27 (21),

13008-13014 DOI: 10.1021/la202792g

[14] Mizutani T, Mizutani A. Estimation of adsorption of drugs and proteins on glass

surfaces with controlled pore glass as a reference. *J Pharm Sci*. 1978

Aug;67(8):1102-5. <https://doi.org/10.1002/jps.2600670820>.

[15] Silva-Bermudez, P., & Rodil, S. E. (2013). An overview of protein adsorption on

metal oxide coatings for biomedical implants. In *Surface and Coatings Technology*

(Vol. 233, pp. 147–158).

[16] P. Cha, A. Krishnan, V.F. Fiore, et al., Interfacial energetics of protein adsorption

from aqueous buffer to surfaces with varying hydrophilicity, *Langmuir*. 24 (2008)

2553–2563. <https://doi.org/10.1021/la703310k>.

[17] J. anne N. Oliver, Y. Su, X. Lu, P.H. Kuo, J. Du, D. Zhu, Bioactive glass coatings

on metallic implants for biomedical applications, *Bioact. Mater*. 4 (2019) 261–270.

<https://doi.org/10.1016/j.bioactmat.2019.09.002>.

- [18] J. Barberi, S. Spriano, Titanium and protein adsorption: An overview of mechanisms and effects of surface features, *Materials (Basel)*. 14 (2021).  
<https://doi.org/10.3390/ma14071590>.
- [19] Visalakshan, Rahul Madathiparambil et al., Biomaterial Surface Hydrophobicity Mediated Serum Protein Adsorption and Immune Responses, *ACS Applied Materials & Interfaces* 2019 11 (31), 27615-27623 DOI: 10.1021/acsami.9b09900
- [20] M.A. Brusatori, Y. Tie, P.R. Van Tassel, Protein adsorption kinetics under an applied electric field: An optical waveguide lightmode spectroscopy study, *Langmuir*. 19 (2003) 5089–5097. <https://doi.org/10.1021/la0269558>.

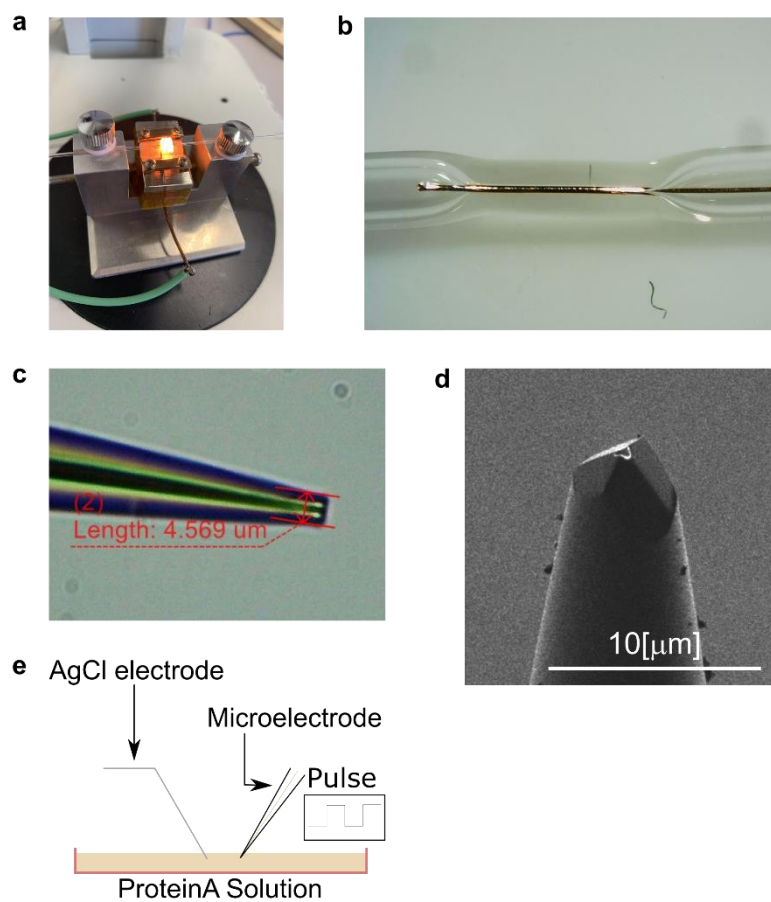


**Fig. 1.** Fabrication Process of Glass Microelectrodes. (a) Heated by the filament of the sealing machine, the gold is sealed inside the glass tube. (b) Sealed glass tube. (c) Glass tube immediately after pulling with a micropipette puller. (d) Tip of a glass tube electrode processed by the FIB system. Scale is 10[ $\mu\text{m}$ ]. (e) Schematic diagram of protein immobilization experiment.

**Table 1.** Program and Filament for Glass microelectrode Fabrication.

Line	Heat	Pull	Vel	Time	Pressure: 500
1x4	510	50	5	0	Preheat: ON
2x2	510	40	5	0	Filament: 220B
3x1	505	0	8	0	Room Temp: 24°C
4x1	505	10	5	0	Humidity: 60%

For Time/Delay setting, Time was selected.

The preheat function is enabled by opening Menu in any program window and checking the [Preheat Jaws 70°C] checkbox. The program will then confirm whether to preheat when it is opened. This function allows the starting temperature to be constant.

Delay Mode is not enabled.

A typical example of an electrode pulled by this program is shown below (Fig S1).



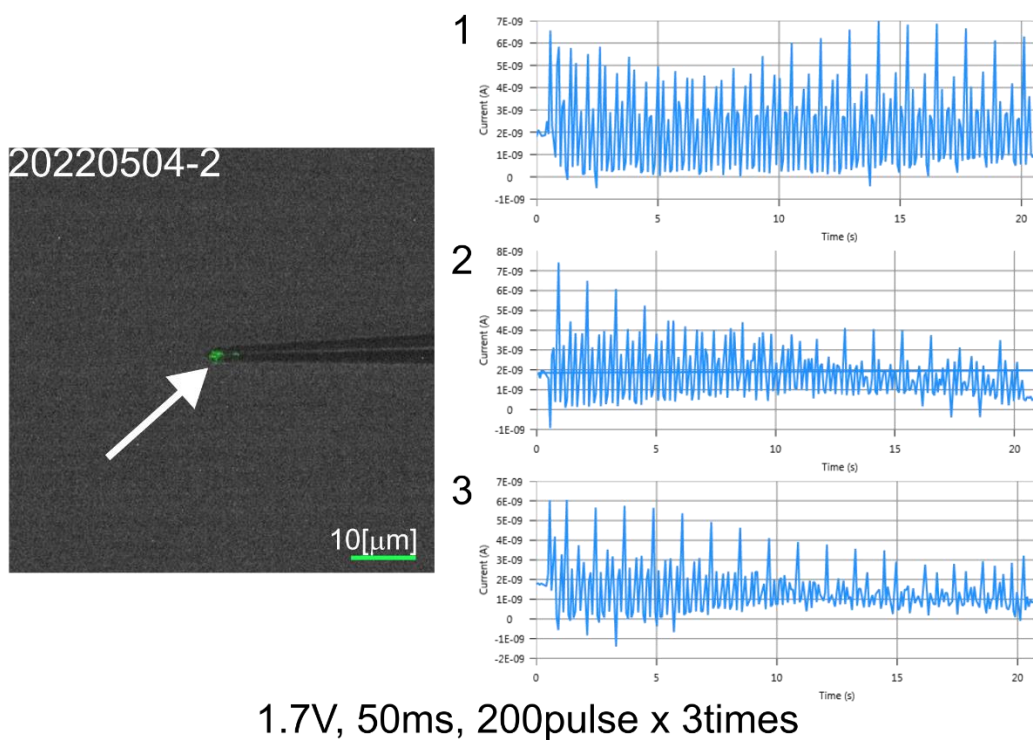
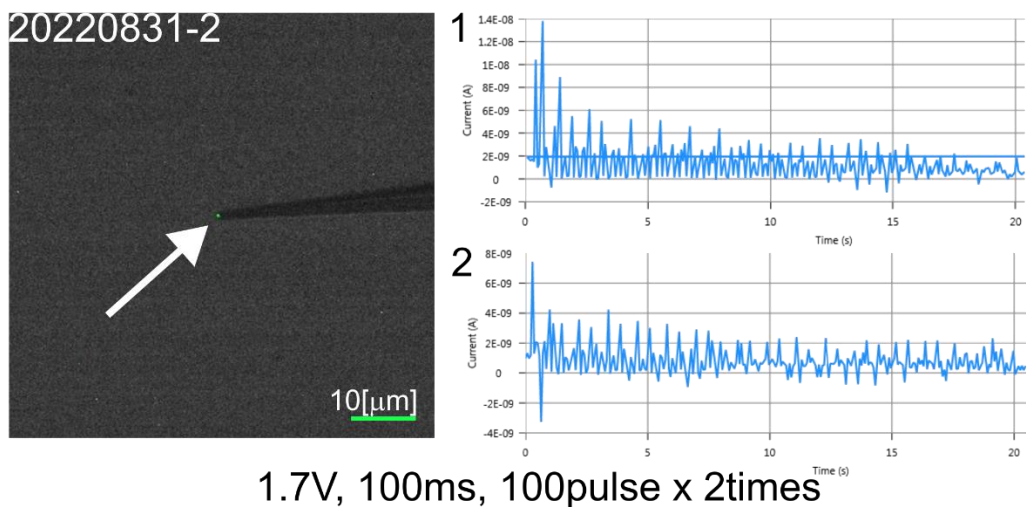
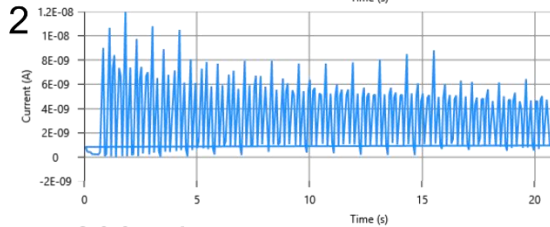
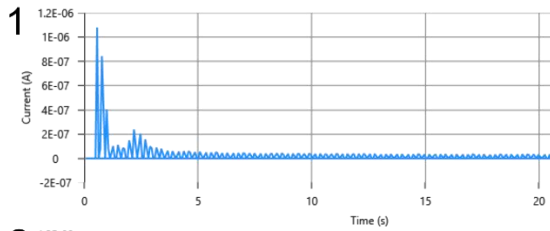
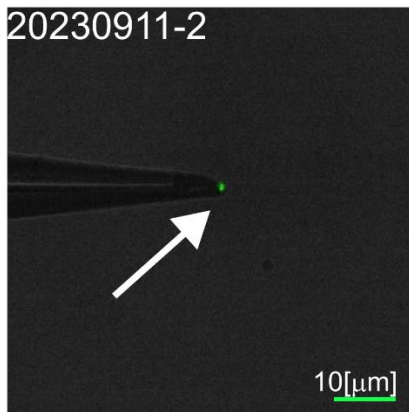
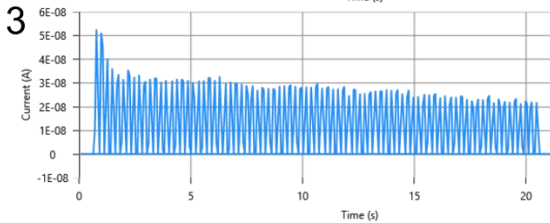
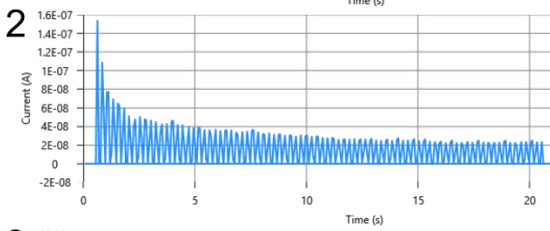
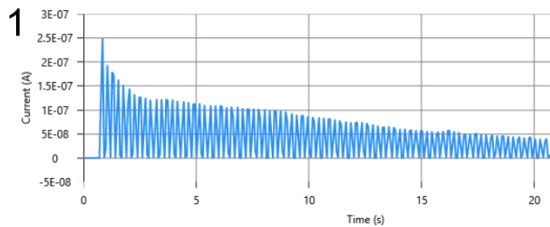
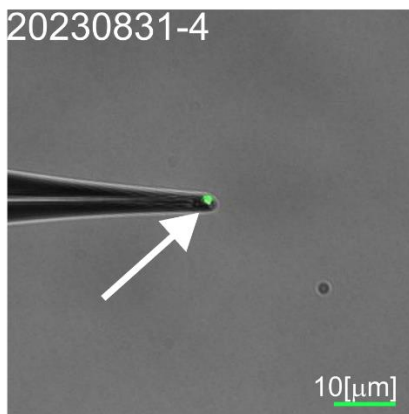


**Fig. 2.** Proteins were immobilized at the tip of the electrode by applying a pulsed voltage. The two experiments differ in pulse interval and frequency. Overnight with Fc-Venus after immobilization of ProteinA (4°C, dark). 20220831-2 is immobilized at the tip, and 20220504-2 is immobilized near the tip, down to the glass area.



1: 2.2V, 50ms, 200pulse  
 2: 2.0V, 50ms, 200pulse



2.1V, 50ms, 200pulse x 3times

**Fig. 3.** Proteins were immobilized at the tip of the electrode by applying a pulsed voltage. The two experiments differ in voltage. Overnight with Fc-Venus after immobilization of ProteinA (4°C, dark). 20230911-2 is immobilized at the tip, and 20230831-4 is immobilized near the tip, down to the glass area.

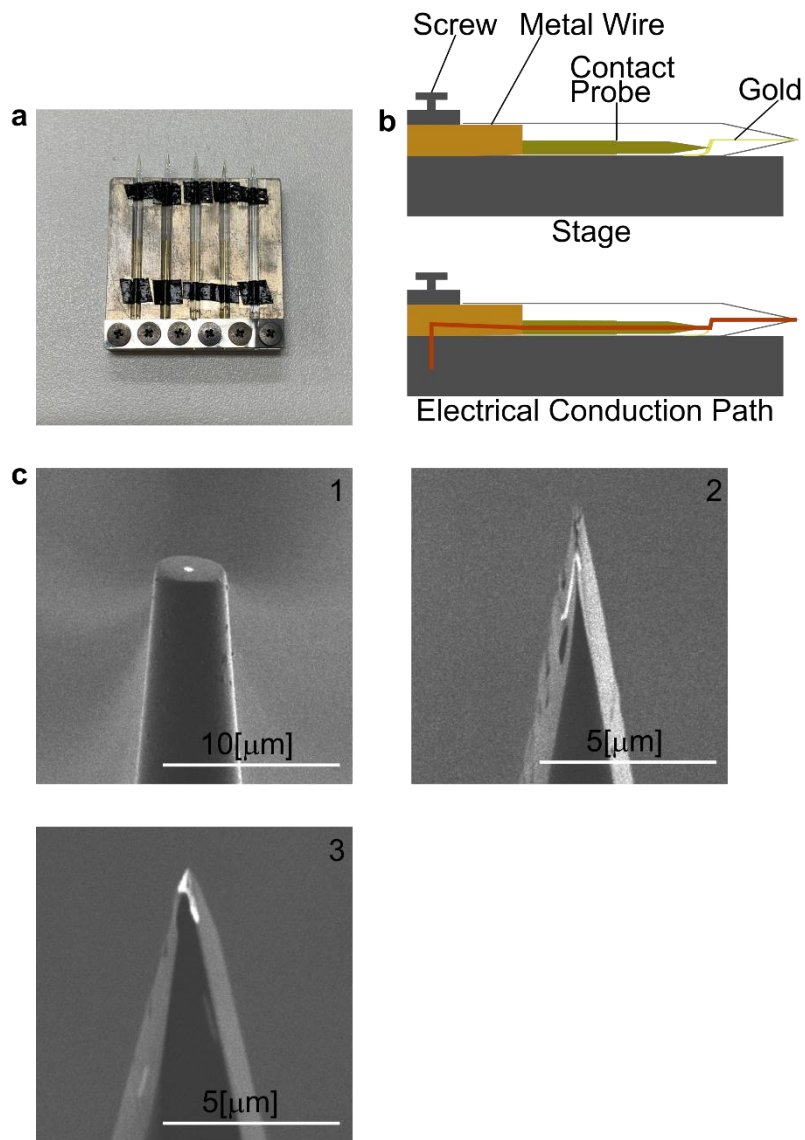


**Fig. 4.** Preparation for FIB processing and FIB processing. (a) 30[mm] square size stage for FIB processing. (b) Side view of the stage (upper). Red lines indicate conduction paths (lower). (c) FIB process flow. (1) Cut horizontally to expose the gold. (2) Cut the left and right sides. (3) Cut again twice at different angles. The pyramidal shape is obtained.

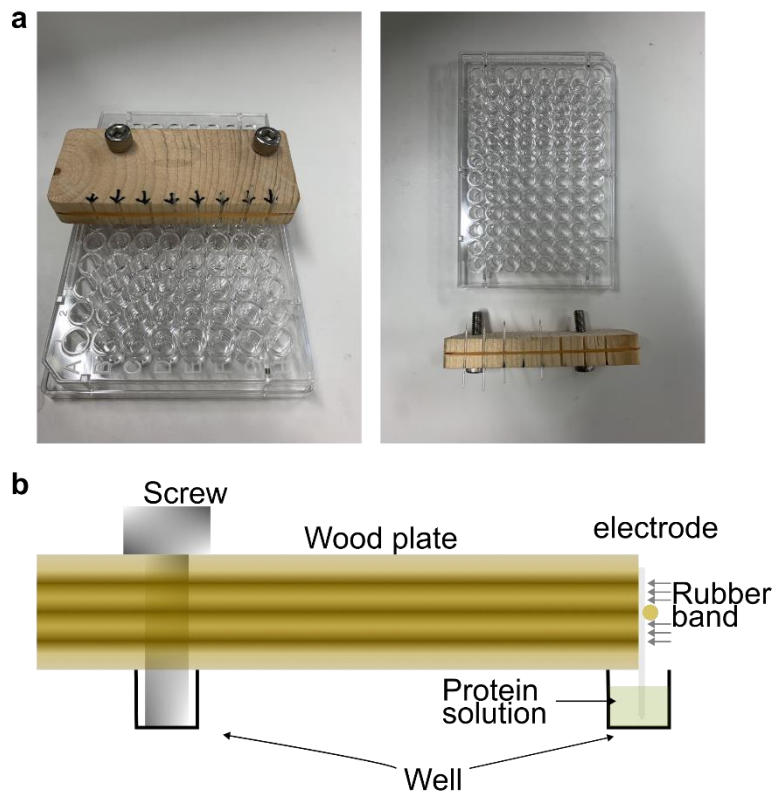


**Fig. 5.** Fixation method for safe oversight of the electrode tip. Electrodes are grabbed with tweezers and secured through rubber bands. Multiple electrodes can be attached at the same time. (a) A wood plate with electrodes fixed with rubber bands and a 96 well plate. By placing two screws in each well and fixing them in place, the entire wood plate is stuck and can be stored for a long time without the tip of the electrode touching the walls or bottom of the well. In use (left) and disassembled (right). (b) Well and wooden board in use (Side view). Electrodes are always pressed by the rubber band.

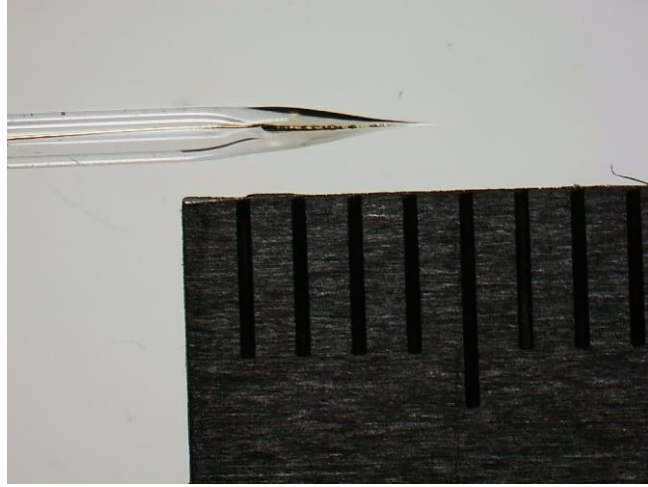


**Fig. S1.** A typical example of an electrode pulled by micropipette puller (Program is shown Table 1). The scale shows 1 [mm]

## Chapter 4

# Proof-of-Principle of Glass Microelectrodes with Selective Synaptic Induction Ability

#### Purpose of Chapter 4

- To induce selective synapse formation using the developed engineered synaptic organizer and glass microelectrodes.

#### Achievement

- Using microglass electrodes on neurons expressing engineered synaptic organizers, the formation of synapses between them was confirmed.

#### Remaining Challenges

- Simultaneous use of several different peptide tags to measure the activity of each genetically different neuron in a neural circuit.

## Chapter 4 Key Points

- The fabricated glass microelectrodes formed synapse-like structures with axons of neurons expressing engineered synapse organizers.
- At least temperature conditions are not essential for culturing chick forebrain neurons in L15, and chick neurons themselves are also easy to culture, making them easier to use in experiments than rat neurons and others.
- Chick forebrain neurons could also be cultured in open air, at room temperature (21 °C), and without a perfusion device, but some necrosis was observed.
- The optimal conditions for the tip shape of the fabricated glass microelectrodes were not known. However, ProteinA was also immobilized on the glass part of the tip, and Rab3 accumulated on the glass part.
- Selective synaptogenesis could be realized by combining the fabricated engineered synapse organizers with glass microelectrodes if experimental conditions were suitable, but the reproducibility was low, leaving room for improvement in many steps.



## **Introduction**

The patch-clamp technique developed by Erwin Neher and Bert Sakmann has made it possible to observe ion channel currents and neuronal activities, including detailed data acquisition of synaptic currents using in vivo patch-clamp recording [1]. Prior to this technique, intracellular electrode techniques were mainly used to obtain current data of cells larger than the electrode tip [1]. After the advent of the patch-clamp technique, cell recording of various techniques has become possible using this technique with greater convenience. This technique has greatly influenced the development of molecular and cell biology and has become a powerful technique in physiology and pharmacology. However, although the patch-clamp technique is a powerful tool that can observe ion channel currents of various cells, it has some problems such as non-destructive observation and low throughput. In addition, the inability to observe networks consisting of multiple cells cannot be ignored today, when detailed data are required for further advanced research.

In Chapter 2, I introduced an engineered synapse organizer consisting of a part of mouse or chicken neurexin-1  $\alpha$  sequence and an N-terminal peptide (SPOT-tag) epitope into Rat neuron and Chick neuron and described the observation of synaptic inductive activity induced from the binding of peptide tag and Nanobody (immobilized on the surface of

microbeads). The formation of synapse, the junction between neurons, was induced in an artificial object, and the inductive activity of synapse by SPOT-tag was observed, indicating that preparation of tags with specific binding (HAT-tag, His-tag, FLAG-tag, etc.) and their antibodies enabled selective synaptic formation with multiple neurons simultaneously [2].

Chapter 3 describes the fabrication of glass microelectrodes with gold cores and the immobilization of functional proteins (mainly ProteinA) on the electrodes. On the other hand, synaptic formation can be induced on the electrode surface by preparing a large number of substrate-type electrodes by lithographic techniques and immobilizing endogenous synapse organizers on the electrode surface, followed by culturing neurons on them. [3] There are also mesh electrodes [4], etc. By using these and engineered synapse organizers, it is possible to perform efficient selective measurement of neurons. The glass microelectrodes with selective synaptic induction ability fabricated in this study can be differentiated from the multiple electrode-type ones described above in the following two ways. One is that the axon of any cell can be approached. The other is that the related equipment (micropipette pullers, manipulators, electrode holders, etc.) used for the existing patch-clamp method can be reused as it is. The first one is different from the existing neuronal measurement methods and multiple substrate-type electrodes

in that it is quite easy to handle. Although the throughput is not expected to change compared with the patch-clamp method, it can be said that it has different advantages considering the possibility of performing measurement with selective neurons via synapses. The substrate-type electrode with multiple electrodes basically has the electrode part fixed, so it cannot be moved, and synaptogenesis is possible only when the corresponding axon approaches the electrode. The second point, that the existing equipment and equipment can be reused, is relatively important for conducting experiments. The glass microelectrodes presented in Chapter 3 are also performed in peripheral equipment used in basic electrophysiology except for tip processing. The fact that the existing equipment can be used from the fabrication to the utilization of the glass microelectrodes means that laboratories using electrophysiological methods can smoothly try these techniques when they can obtain more versatility and stability. If I can provide a new potential method without major changes compared with the existing method, the pace of feedback will be faster, so I expect to further improve the method proposed in this study.

In this chapter, I conduct proof-of-principle experiments on a glass microelectrode with such a background and show by proof-of-principle experiments that the developed glass microelectrode with an engineered synapse organizer immobilized has selective

synaptic induction ability.

## **Materials and Methods**

To demonstrate the principle, I basically used the materials and methods used in Chapters 2 and 3. First, I prepared chick neurons cultured in L15 (CO<sub>2</sub>-independent) at 37 °C. Chick forebrain neurons were prepared by culturing fertilized eggs purchased from vendors at 38 °C for 8-9 days. Since the culture experiments and preparation experiments using L15 conducted in Chapter 2 showed that the culture in open air and at room temperature was possible for at least 24 hours, I conducted the experiment using the same L15 culture as presented in Chapter 2 (L15, 2% HS or FBS). The other culture conditions were the same as those presented in Chapter 2, but the glass for culturing neurons was changed to one with a size of 18 mm (No. 1. Matsunami), it was coated with a mixture of 1.0mg/ml PLL and 0.1mg/ml PDL, and Chick forebrain neurons were cultured by the method described in Chapter 2. Then, the neurons were transfected with the engineered synapse organizer produced and evaluated in Chapter 2 on the 4th day from the start-up and observed by fluorescence 1 day later. The neurons thus prepared were transferred under a microscope (IX71) and observed by fluorescence in L15 culture as previously described.

The microscope and CCD camera, etc. are basically the same as in Chapter 3. The appearance of the experimental environment (**Fig. 1**). The glass microelectrode with synaptic inductive ability produced in Chapter 3 was approached to the axon of the neuron transfected the engineered synapse organizer we developed. The necessity of the perfusion equipment and the temperature conditions were examined using the perfusion equipment and the temperature controller (TC-324B, Warner Instruments) so that the neuron would not be deactivated during observation for more than 8 hours. Since the only difference compared with the experiment using microbeads used in Chapter 2 is that the microelectrode was cultured in open air and at room temperature, basically the same data would be expected to be obtained. Therefore, I confirmed that the same synaptogenesis could be seen by experimenting with the microbead used in Chapter 2 in co-culture at the same time as the microelectrode produced.

The data obtained were compared and examined. The combination of fluorescence filters used was the same as in Chapter 3. Excitation and emission filters were selected according to the fluorescent proteins (EGFP, mcherry) attached to Rab3 at the N-terminus of the engineered synapse organizer. The data were acquired using IDL (Research Systems, USA) and analyzed using ImageJ.

## Results

First, I performed an experiment using a perfusion apparatus in which the temperature of cultured neurons under the microscope was kept constant at 31.6 °C. The culture medium was L15, HS2%, and chick forebrain neurons could be cultured using this culture medium in the incubator without any problems (**Fig. 2**). Therefore, the temperature was lower than the preset temperature of the incubator (37 °C). Compared with the previous L15 culture, the open-air culture was the most different. However, not all neurons remained active after culturing at room temperature (about 21 °C) without the heater, and some cells were found dead after culturing for at least 9 h (**Fig. 3**). However, even under the conditions of L15 HS2%, room temperature (about 21 °C) without the perfusion apparatus, fluorescence representing the accumulation of Rab3 was confirmed on the microbeads on which the antibodies of the engineered synapse organizers were modified (**Fig. 4**). In order to perform the experiment more stably, I decided to perform the L15, FBS2%, room temperature (about 21 °C) with the perfusion apparatus. As a result of the previous room-temperature co-culture experiment of L15 and microbeads, the accumulation of EGFP-Rab3 on the microbeads was confirmed as in other experiments (**Fig S1**). In the system using L15, FBS2%, and the perfusion apparatus, the cells were able to be active for at least 8 h, and the accumulation of Rab3 on the tips of the electrodes was confirmed. The

axon and dendrite rupture, which are common in neurons just before collapse, were not observed (**Fig. 5**). Based on the above experimental results, I can say that the FcBC2Nanobody immobilized on the tips of the electrodes combined with the engineered synapse organizers with the SPOT tag, and the synapse-like structure could be induced by the accumulation of Rab3 and the confirmation of Synapsin localization performed in Chapter 2. However, due to the characteristics of the experiment, I must also mention an example of failure. Here, I introduce a typical experimental failure that occurred during an experiment using glass microelectrodes (**Fig. 6**). In general, the successful fabrication and processing of glass microelectrodes and the successful culture experiment using chick neurons can provide various data, but it cannot be denied that there are many problems to be solved in the future, such as the destruction of the electrodes and the failure of culture.

## **Discussion**

In this chapter, I found that engineered synapse organizers were able to bind to the tips of ProteinA-mediated Anti-SpotNb-immobilized glass microelectrodes and induce the formation of synapses on the tips of the electrodes. This finding allowed us to find that measuring with the fabricated glass microelectrodes can be a method for measuring electrophysiology through synapses and that the fabricated engineered synapse organizers

work with chick neurons, making it possible to measure with the combination of multiple independent synapse organizers [5]. Looking at Figure 6, I found that Rab3 was assembled in the glass part at the tip of the electrodes, but this could be improved by increasing the surface area of the gold at the tip. In addition, although the addition of FBS to the culture medium and the use of a perfusion device could relatively improve the culture condition of neurons, culturing chick forebrain neurons on a microelectrode array and co-culturing with glial cells could potentially lengthen the neuron cells [6].

On the other hand, to control the immobilization of ProteinA, which is a problem with glass microelectrodes, it seems to be more effective to use a method in which the exposed area of gold is adjusted by plating gold on the electrode tip than in the previous study [3].

In addition, it is likely that electrode tip breakage and electrode shaking, which were problems in the experiments conducted in this chapter, can be dealt with by improving the environment around the manipulator and the microscope. In general, although highly reproducible results were not obtained, the fabricated engineered synapse organizers and glass microelectrodes were able to contact cultured neurons and form synapse-like structures. Thus, it can be said that the technology that will be the basis of the microelectrode technology for neuronal activity recording for the next generation with cell recognition function has been established. In the future, I will analyze the quantitative



data of the engineered synapse organizers discussed in Chapter 2, elucidate the molecular mechanism on synapse induction, and improve the glass microelectrode fabrication method presented in Chapter 3, in order to establish cell activity measurement via synapses and selective multiple simultaneous measurement of neurons.

## References

- [1] T. Ishikawa, M. Shimuta, M. Häuser, Multimodal sensory integration in single cerebellar granule cells in vivo, *Elife*. 4 (2015) 1–10. <https://doi.org/10.7554/eLife.12916>.
- [2] K. Terpe, Overview of tag protein fusions: From molecular and biochemical fundamentals to commercial systems, *Appl. Microbiol. Biotechnol.* 60 (2003) 523–533. <https://doi.org/10.1007/s00253-002-1158-6>.
- [3] S. Kim, M. Imayasu, T. Yoshida, H. Tsutsui, Formation of neuron-microelectrode junction mediated by a synapse organizer, *Appl. Phys. Express*. 16 (2023). <https://doi.org/10.35848/1882-0786/acd166>.
- [4] T.M. Fu, G. Hong, R.D. Viveros, et al., Highly scalable multichannel mesh electronics for stable chronic brain electrophysiology, *Proc. Natl. Acad. Sci. U. S. A.* 114 (2017) E10046–E10055. <https://doi.org/10.1073/pnas.1717695114>.
- [5] S.A. Hamid, M. Imayasu, T. Yoshida, et al., Epitope-tag-mediated synaptogenic activity in an engineered neurexin-1  $\square$  lacking the binding interface with neuroligin-1, *Biochem. Biophys. Res. Commun.* 658 (2023) 141–147. <https://doi.org/10.1016/j.bbrc.2023.03.063>.
- [6] S.Y. Kuang, Z. Wang, T. Huang, et al., Prolonging life in chick forebrain-neuron culture and acquiring spontaneous spiking activity on a microelectrode array, *Biotechnol. Lett.* 37 (2015) 499–509. <https://doi.org/10.1007/s10529-014-1704-1>.

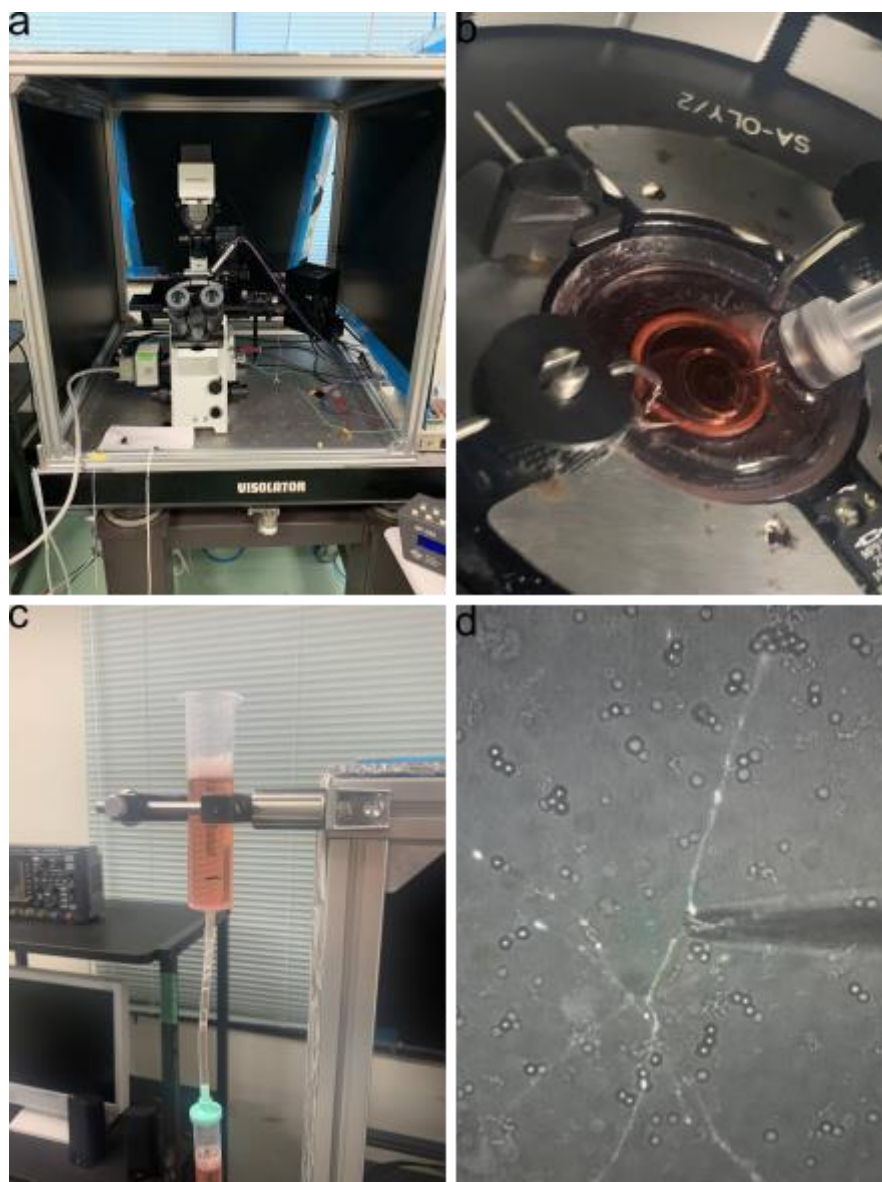


**Fig. 1.** Appearance of the experimental environment. (a) The area around the microscope, including the irrigation system, manipulators for electrode manipulation, and wiring for heaters. (b) A glass plate containing a Chick neuron culture is placed above the microscope lens. An electrode is approaching from the right. (c) L15 culture medium being pumped by the perfusion system. (d) Typical neuron in this environment. The electrode is in contact with the axon.

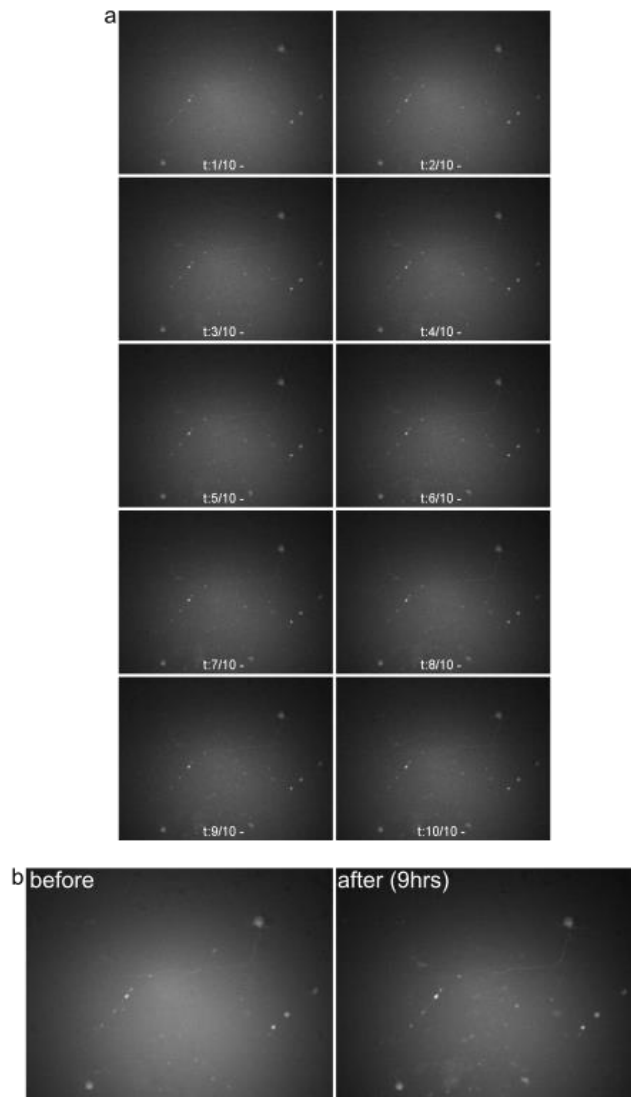


**Fig. 2.** L15, HS2%, 31.6°C and with perfusion. Chick neuron cultured under a microscope. (a) Photos taken every hour for about 9 hours of incubation. (b) Comparison between immediately after the start of cultured and 9 hours later.

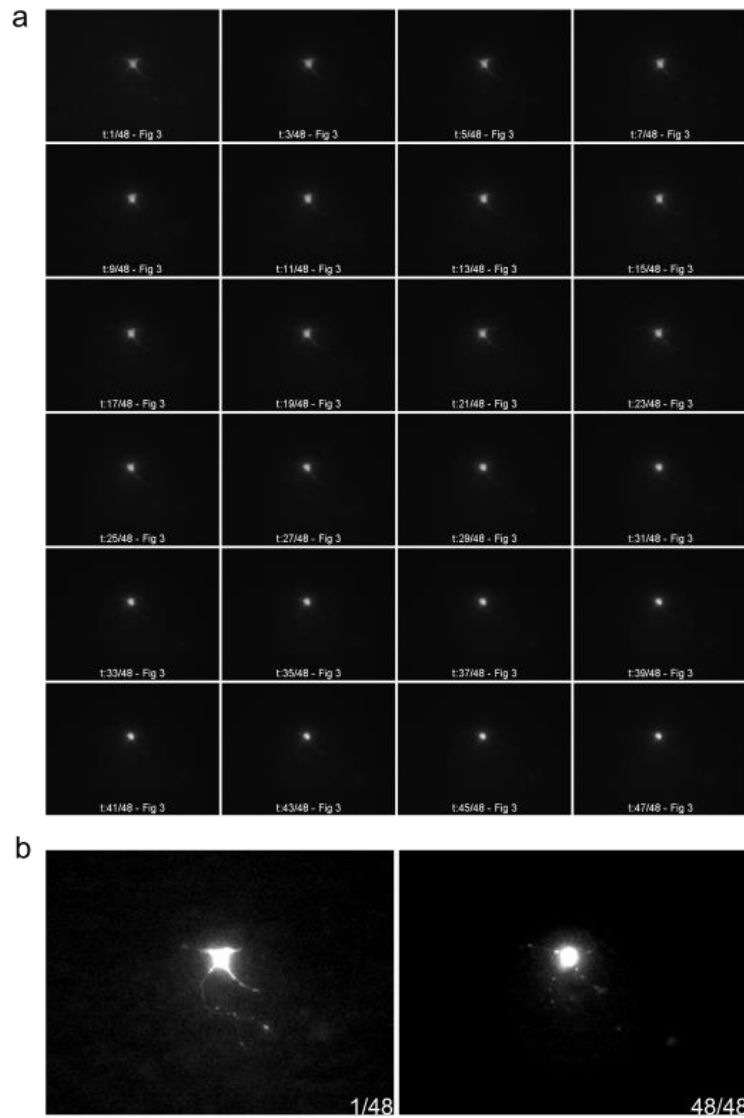


**Fig. 3.** L15, HS2%, 21°C (no heater) and without perfusion. Chick neuron cultured under a microscope. Neuron incubated in L15, HS2% for 480 minutes were photographed every 10 minutes. (a) Photos were taken every 10 minutes from the start of incubation. (b) Immediately after the start of the post-incubation imaging and 8 hrs later.

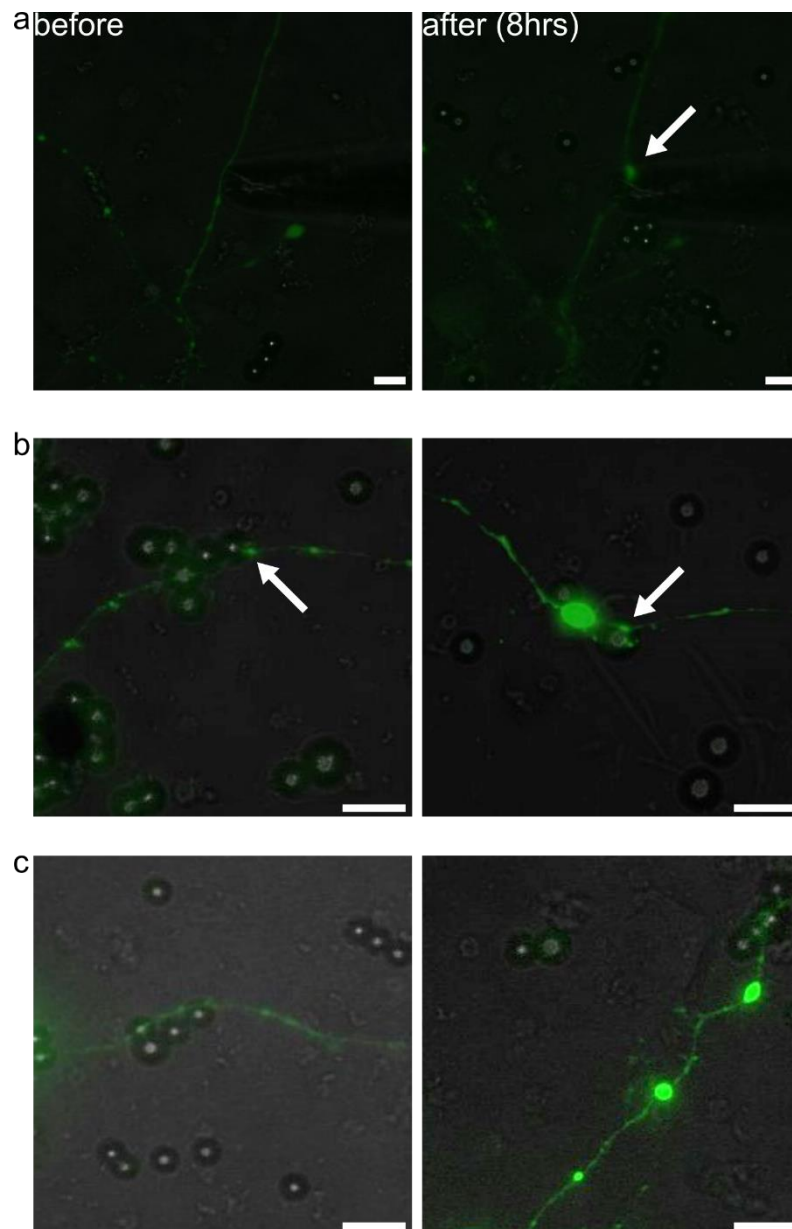


**Fig. 4.** Chick neurons were cultured in L15 (HS 2%) in room temperature (21°C), without perfusion observed fluorescently. (a) Glass microelectrodes were contacted with axons of neurons expressing engineered synapse organizers. The accumulation of EGFP-Rab3 was confirmed at the tip of the electrode after 8 hours at the latest. (b) Chick neurons and Nanobody-immobilized microbeads were co-cultured for 8 h. The accumulation of EGFP-Rab3 was confirmed in surface of the microbeads (except for the culture environment, the conditions were the same as those shown in Chapter 2, Fig 4). (c) Control beads were used under the same conditions as in (a) and (b), but no EGFP-Rab3 was accumulated on the microbeads. Bars = 10  $\mu$ m.

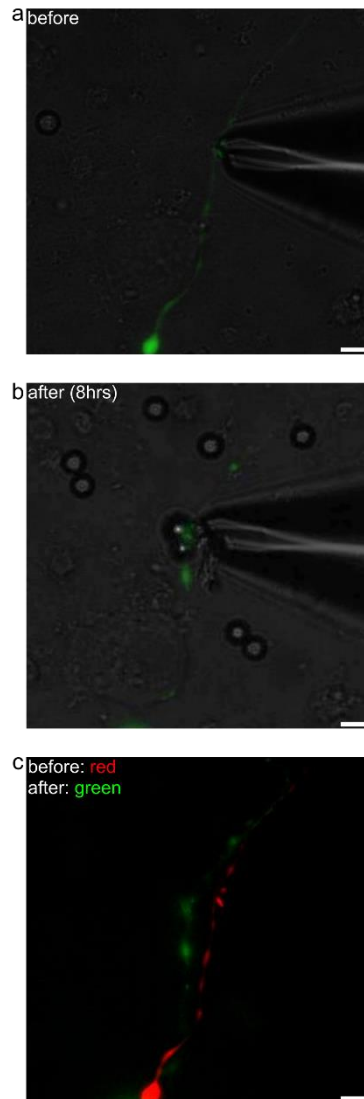


**Fig. 5.** Chick neurons could be successfully cultured in L15, FBS 2% using a perfusion device (co-cultured with bare-microbeads). (a) Immediately after the start of culture, the tip of the electrode was contacted with axon. (b) After 8 hours, Rab3 accumulation was observed at the electrode tip. (c) Fluorescence showing the accumulation of Rab3 at the beginning of the observation (red) and 8 hours later (green).

Bars = 5  $\mu\text{m}$ .

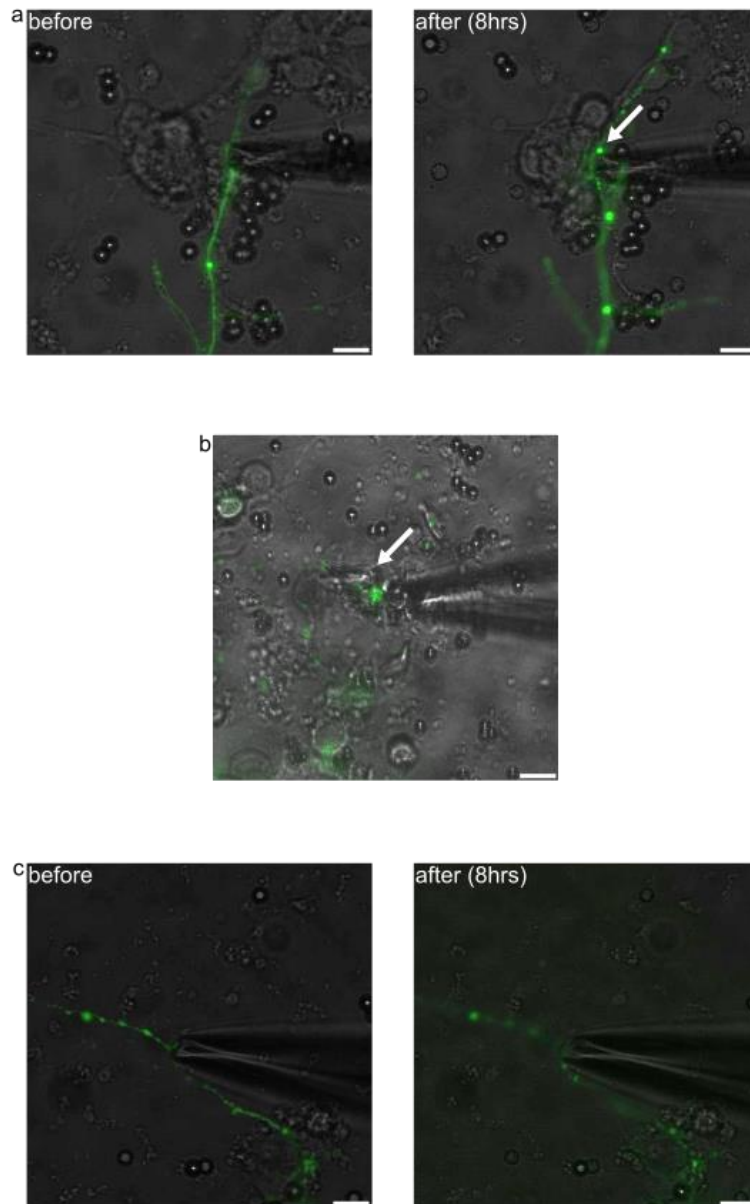


**Fig. 6.** Typical failure of an experiment using glass microelectrodes. (a) Rab3 (modified with fluorescent protein) accumulated on the non-gold tip of the electrode. (b) The tip of the electrode touched the bottom and was broken. (c) The slight movement of the electrode during 8 hours of incubation prevents it from contacting the axon (out of focus). Bars = 10  $\mu\text{m}$ .



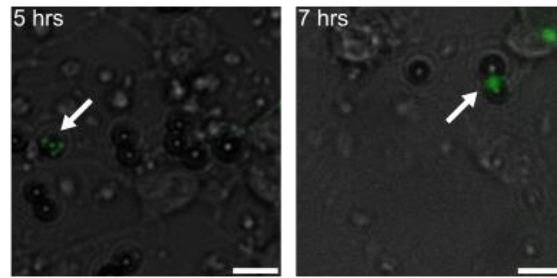


**Fig. S1.** Microbeads modified with a tag that binds to the engineered synapse organizer were co-cultured with transfected chick neurons. The neurons were co-incubated for approximately 5 and 7 hours in room temperature (21°C), respectively. EGFP-Rab3 (green fluorescence, arrow) accumulates on the surface of microbeads. Bars = 10  $\mu$ m.

# General Discussion

### Achievement

- By using microelectrodes with specially processed tips, synaptogenesis could be induced in specific neurons expressing engineered synapse organizers.

- Remaining Challenges

Improving efficiency of synapse formation experiments with engineered synapse organizers and the microelectrodes.

In this study, I developed and quantitatively evaluated an engineered synaptic organizer based on Mouse, Chick NRXN-1 $\beta$ , and developed glass microelectrodes to approach the axons of neurons. Proof-of-principle experiments were conducted using a combination of these techniques.

Innumerable neurons in the brain are connected by synapses to form a huge network for information transmission and computation. Information transmission and processing by complex neural circuits by normally differentiated and active neurons generate various behaviors in living organisms. In general, synapses are required to be connected by synapses to other neurons and muscles, and neurons grow to transmit information to other cells while extending axons. Neurons that reach their target cells and initiate synaptic differentiation receive information from dendrites themselves and participate in the development and maintenance of the normal network, becoming one element of the neural circuit architecture.

It has recently become clear that proteins called synapse organizers are involved in the formation of synapses, and research has been actively conducted to elucidate the mechanism. Many synapse organizers have a huge number of subfamilies formed by alternative splicing, and it is thought that the realization of innumerable modes of connection enables control of normal synapse formation and maintenance. Neurexin

(NRXN) and Neuroligin (NLGN), a pair of synapse organizers, have been known for a long time, and they are located in the presynaptic and postsynaptic regions, respectively. It is thought that their intercellular connection promotes the dimerization of NLGN and the clustering of NRXN, thereby initiating presynaptic differentiation.

Based on this idea, this study attempted to develop and apply a device using an engineered synapse organizer that lacks the LNS of NRXN-1 $\beta$  and has a Spot-tag at the N-terminus. LNS is the extracellular domain of NRXN and has been shown to bind NLGN with nanomolar affinity. Prior studies have shown that synaptogenesis can be induced by artificial binding even in the absence of this endogenous binding site.

Therefore, the application of such molecular tools to glass microelectrodes opens up the possibility of measuring neuronal activity, which was not possible before. Selective measurement of neuronal activity is not possible with patch clamp or extracellular electrode methods, and synapse-mediated measurement is an unprecedented method.

Selective measurement of neuronal activity allows us to obtain data focused on specific neuronal activity within a neural circuit, from which a new understanding of neural circuits is likely to emerge. Therefore, we developed a glass microelectrode with synaptic induction capability using the engineered synaptic organizer we developed, and conducted a proof-of-principle experiment. Glass microelectrodes are microelectrodes

with gold sealed inside and insulated with glass, similar to those used in the patch-clamp method. Although the performance of the fabricated electrodes has not been evaluated, it is known from the experiments described in Chapter 3 that current can flow. Experiments using microbeads and engineered synaptic organizers showed that synapse-like structures can be selectively formed. However, it is not clear whether synapses formed by this mechanism have normal function or excitatory and inhibitory properties. When microbeads and the tips of glass microelectrodes modified with Spot-tag and Nanobody were attached to engineered synaptic organizers, both showed accumulation of Rab3 (a synaptic marker).

Future perspectives include the measurement of signals from synapses created on the tip of glass microelectrodes. To achieve this, the following items must be achieved.

The first is the characterization of electrodes. It has been found that the developed electrodes carry a current of at most several hundred nanoampere when 1.7 to 2.0 [V] is applied to them. It is essential to investigate the characteristics of the electrodes in order to create a dedicated amplifier and to clearly read the signals.

The second is the development of more efficient electrodes and the probability of synaptic-guided experiments. The development of electrodes was made efficient through the processing of universal machines, but this was not the case with tip

processing. In order to repeat experiments using electrodes as described in Chapter 4 and to perform experiments with high efficiency, the electrode processing process and the method of contacting axons must be revised.

The third is the probability of synaptic-mediated measurement methods. As shown in previous studies (S. Kim et al., 2023), two types of measurement methods can be considered for the measurement of created synapses. One is through capacitive coupling, and the other is by electrochemically sensing and reading the release of neurotransmitters.

The first described method is ideal, and if the signal can be detected through direct electrical coupling between a neuron and a microelectrode, it may be possible to measure using an amplifier similar to the patch-clamp method. However, as previously described, the amplifier must be adjusted to the characteristics of the electrodes.

If these are achieved and selective synaptogenesis induction and neuronal signal acquisition can be achieved, the signal of a specific neuron in a neuronal circuit can be tracked, which will lead to the elucidation of the mechanism of a neuronal circuit. In the brain, neurons are thought to be indispensable for complex activities and behavioral decisions due to their diversity, and a myriad of neuronal circuit assemblies construct higher-order functions. Therefore, the elucidation of the function of a neuron in a

neuronal circuit is thought to benefit the elucidation at the functional unit level of the brain. The elucidation of the mechanism of the brain is an imperative proposition, and the unknown function elucidation of neurons, synapses, and neuronal circuits obtained in the process will surely become important information to be utilized in a wide range of fields such as medical treatment and brain science.



# Acknowledgements

I would like to express my sincere gratitude to my supervisor Professor Dr. Hidekazu Tsutsui, Area of Bioscience and Biotechnology (JAIST) for all the guidance he gave me in conducting this research. I would also like to express my gratitude to my associate supervisor, Mr. Goro Mizutani, for his constant support in important situations. I sincerely appreciate Dr. Yuichi Hiratsuka's generous support and advice as an advisor for Minor research and for his technical assistance. I would like to thank Ms. Mieko Imayasu for her many experimental aids. I am deeply grateful to the Japan Advanced Institute of Science and Technology (JAIST) for funding a Doctoral research Fellowship (DRF). I am grateful to the members of our laboratory and the staff of JAIST's Nanomaterials Technology Center, especially Ms. Ito, for their support. Lastly, I give my heartfelt thanks to my family and my grandparents.